

***Development of probiotics and alternative treatments for
stony coral tissue loss disease***

Final Report of Task 2 and Task 3

Prepared By:

Valerie J. Paul, Blake Ushijima, Kelly Pitts

Smithsonian Marine Station at Fort Pierce
701 Seaway Drive
Ft. Pierce, FL 34949

Neha Garg
School of Chemistry and Biochemistry
Georgia Institute of Technology
Atlanta, GA 30332

August 31, 2020

Introduction

A disease, termed stony coral tissue loss disease (SCTLD), throughout the Florida Reef Tract (FRT) has resulted in massive die-offs of over 20 of the known 45 species of scleractinian corals in Florida. This disease has proven highly virulent forcing some highly susceptible species into local extinction. While the Caribbean has been known as a hotspot of coral diseases, SCTLD is particularly of great concern because of its spatial and temporal range and impact on numerous species. In six years, the SCTLD outbreak has spread to extend the majority of the FRT and has additionally been reported in Jamaica, Mexico, Belize, Sint Maarten, Sint Eustasius, Puerto Rico, the Bahamas, the Dominican Republic, the Turks and Caicos Islands, and the Virgin Islands.

An investigation of beneficial microorganisms that inhibit targeted bacteria cultured from diseased corals was conducted in 2018-2019. Preliminary results demonstrated the effectiveness of probiotic McH1-7 at stopping SCTLD progression and preventing infection in laboratory aquaria. Additionally, the examination of the relationship of *Vibrio coralliilyticus* to SCTLD suggested that this bacterial species may be involved in coinfections, which may be causing the variability seen in disease lesions.

The overall goals of this project are: 1) to further develop multi-strain probiotic treatments and to identify additional potential probiotics, and 2) to test alternative treatments and diagnostic tools to complement probiotic treatments.

Task 2 To further develop multi-strain probiotic treatments and to identify additional potential probiotics.

Effectiveness of probiotic McH1-7 at treating infected *Montastraea cavernosa* colonies

Initial examination of probiotic McH1-7 conducted from 2018-2019 demonstrated the effectiveness of this strain to treat *M. cavernosa* colonies infected with SCTLD. As such, this investigation was continued on coral colonies by inoculating diseased fragments in aquaria with McH1-7 and monitoring disease progression over 21 days. All diseased fragments treated with McH1-7 and diseased control fragments of the same genotype treated with filtered seawater (FSW) were photographed daily and the percentage of healthy tissue remaining over time was calculated (Fig. 1A). The percent tissue was calculated to normalize the data for the differences in coral fragment size and initial starting tissue. The resulting area under the curve (AUC) was compared between treatments (Fig. 1B; paired t-test: $p < 0.0001$, $n = 22$) with a larger AUC corresponding to slower disease progression. Kaplan-Meier survival curves were plotted and a log-rank (Mantel-Cox) test determined that survival was significantly higher with the McH1-7 treatment (Fig. 2; $p = 0.035$, $n = 22$). Note, this analysis does not differentiate between lesions that have arrested and diseased fragments that progressed but did not completely die within 21 days. Overall, it has been concluded that probiotic McH1-7 is an effective treatment for SCTLD on infected *M. cavernosa* colonies *ex situ*.

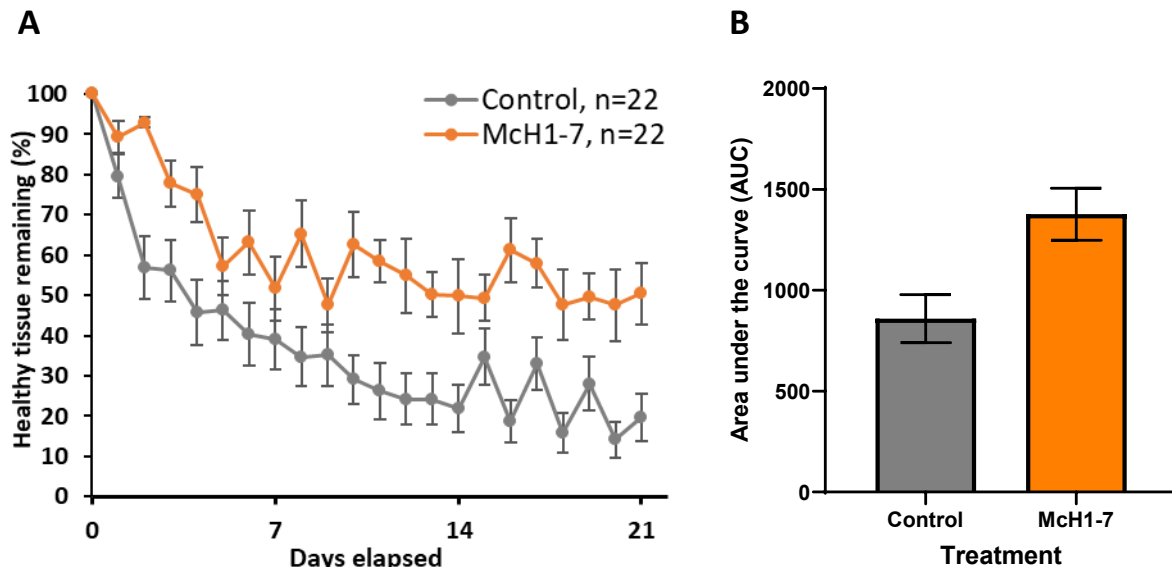


Figure 1. A) Percentage (mean \pm SE) of healthy tissue remaining on infected *Montastraea cavernosa* fragments treated with McH1-7 or FSW (control) and B) subsequent Area Under Curve (AUC) with a larger AUC corresponding to slower disease progression. Data are shown as mean \pm 1 standard error of the mean (SEM).

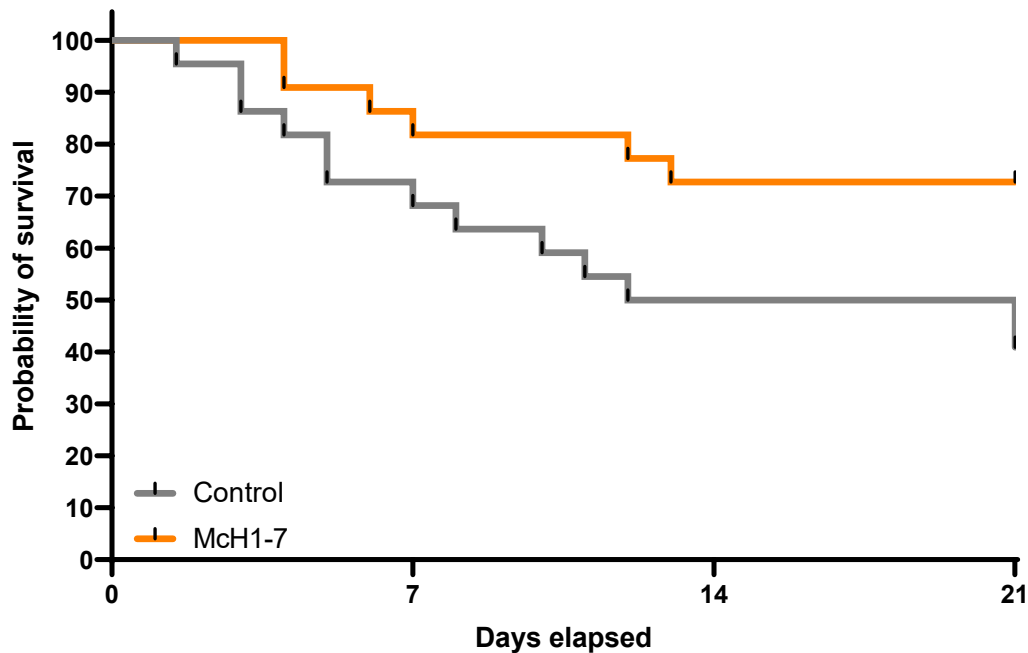


Figure 2. Kaplan–Meier survival analysis of the probability of survival of diseased *M. cavernosa* fragments of the same genotype treated with McH1-7 or FSW (control) over time. Survival Log-rank (Mantel-Cox) test: $p = 0.035$, $n = 22$.

To continue screening of potentially resistant corals for potential probiotics.

Over 2,000 isolates have been collected from apparently healthy or disease resistant coral colonies. Four hundred of these isolates have been screened for antibacterial activity in attempt to find potential probiotics. To do so, putative pathogens were assayed against three isolates (including *Vibrio coralliilyticus*) via plate-based assays. In short, liquid cultures of potential probiotics were spotted onto a plate of growth media previously spread with a culture of a potential pathogen. If the potential probiotic inhibited the growth of the putative pathogen, it was further characterized by chemical analysis and genomic sequencing (see below).

Effectiveness of probiotic Of7M-16 at treating infected Orbicella faveolata colonies

A potential probiotic strain isolated from healthy *Orbicella faveolata*, Of7M-16, produced multiple antibacterial compounds and was therefore tested on diseased *O. faveolata* fragments in aquaria. A total of 12 genotypes of diseased *O. faveolata* were each split evenly into 2 fragments to be treated with Of7M-16 or FSW (control). All colonies were monitored and photographed over 21 days and the percentage of healthy tissue remaining over time was calculated (Fig. 3A). The resulting area under the curve (AUC) was compared between treatments (Fig. 3B; paired t-test: $p = 0.078$, $n = 12$). A log-rank (Mantel-Cox) test was conducted to compare the probability of survival between treatments over time (Fig. 4; $p = 0.252$, $n = 12$). However, differences were not statistically significant, suggesting Of7M-16 is not an effective treatment for infected *O.*

faveolata. These results suggest that Of7M-16 may not be a probiotic, but exposure to this bacterium was not detrimental to *O. faveolata*.

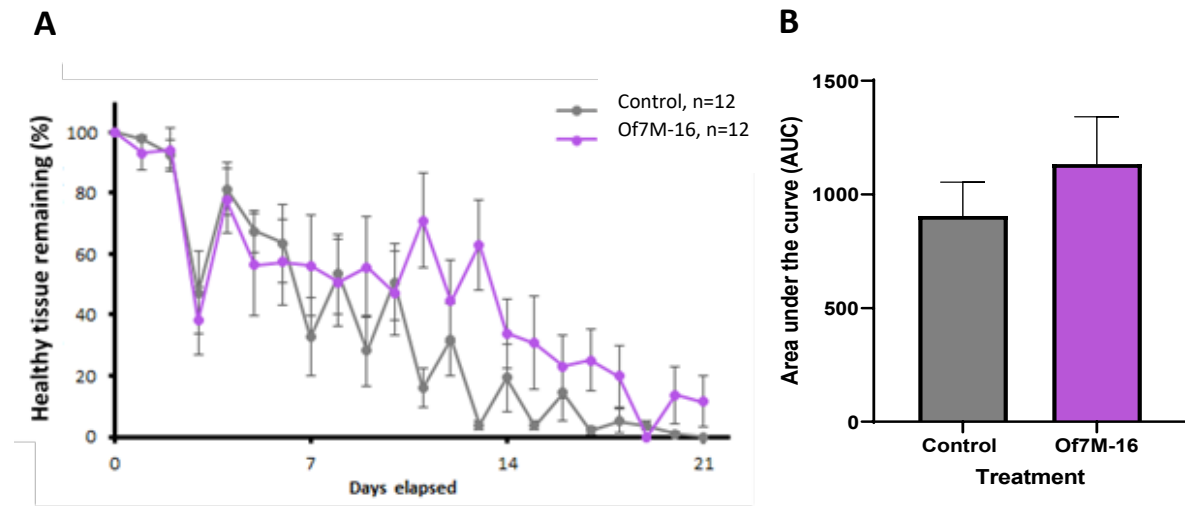


Figure 3. A) Percentage (mean \pm SE) of healthy tissue remaining on infected *O. faveolata* fragments treated with Of7M-16 or FSW (control) and B) subsequent AUC with a larger AUC corresponding to slower disease progression. Data are shown as mean \pm 1SEM.

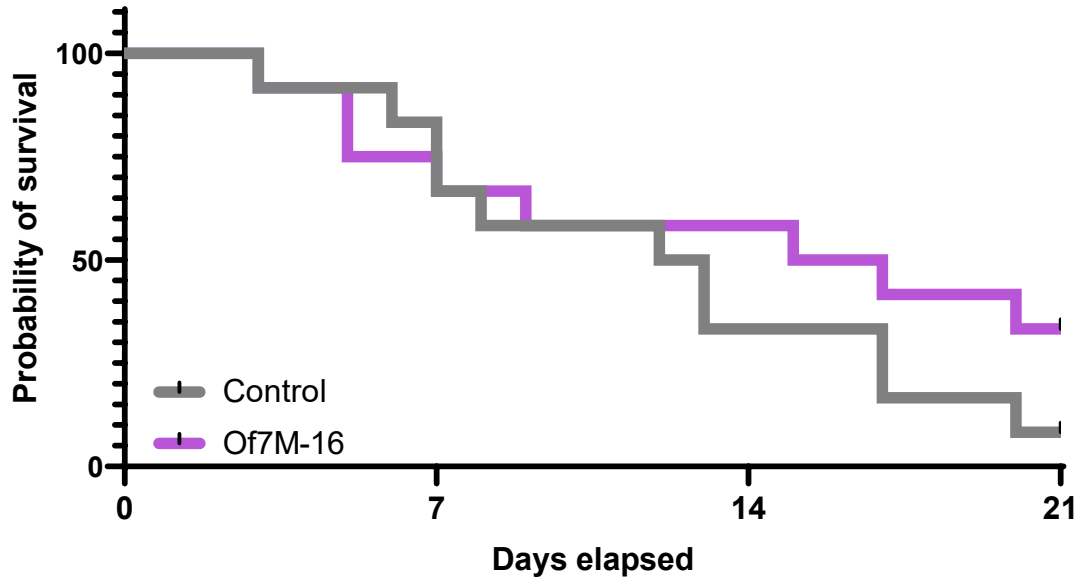


Figure 4. Kaplan–Meier survival analysis of the probability of survival of diseased *O. faveolata* fragments of the same genotype treated with Of7M-16 or FSW (control) over time.

Effectiveness of probiotic McH1-7 at treating infected *O. faveolata* colonies

There are various pros and cons to probiotic treatments that are specific to certain species of coral; however, the effective range of our most effective probiotic McH1-7 was unclear. Therefore, the effectiveness of McH1-7 on *O. faveolata* colonies was investigated. A total of 9 *O. faveolata* genotypes were each split into 3 fragments and then treated with McH1-7, Of7M-16 or FSW (control). All colonies were monitored and photographed over 21 days. The percentage of healthy tissue remaining over time was calculated (Fig. 5A) and the subsequent AUC was compared between treatments (Fig. 5B; repeated measures ANOVA: $p = 0.101$, $n = 9$). A survival log-rank (Mantel-Cox) test compared the probability of survival between treatments over time (Fig. 6; $p = 0.278$, $n = 9$). Of7M-16 slowed or stopped disease progression on 4 fragments whereas McH1-7 slowed or stopped progression on 3 fragments out of 9 total genotypes treated. Differences between treatments were not significant suggesting McH1-7 may not be as effective on *O. faveolata* compared to *M. cavernosa*.

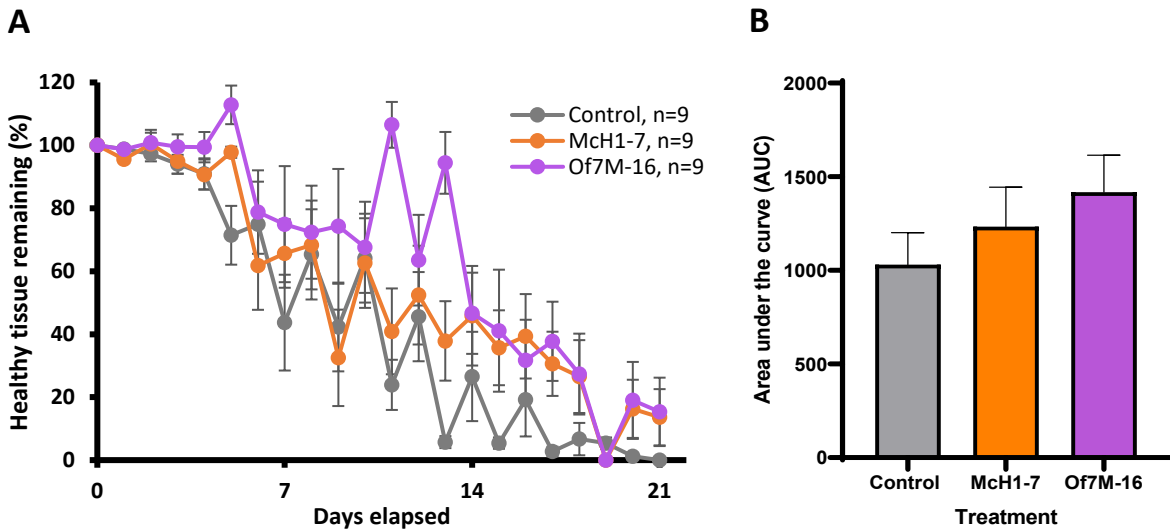


Figure 5. A) Percentage (mean \pm SE) of healthy tissue remaining on infected *O. faveolata* fragments treated with Of7M-16, McH1-7 or FSW (control) and B) subsequent AUC with a larger AUC corresponding to slower disease progression. Data are shown as mean \pm 1SEM.

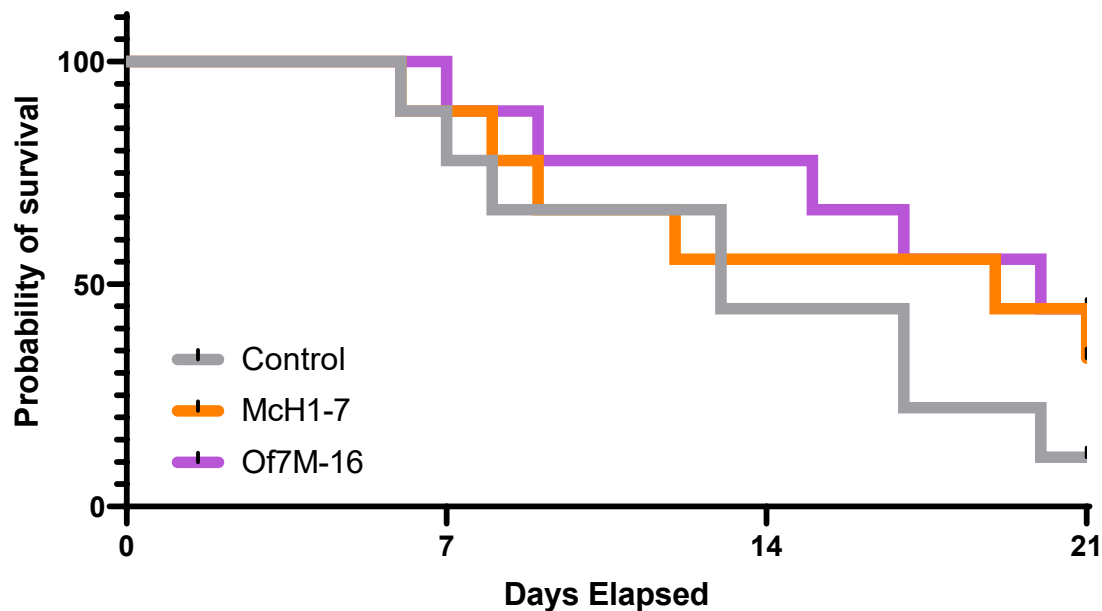


Figure 6. Kaplan–Meier survival analysis of the probability of survival of diseased *O. faveolata* fragments of the same genotype treated with Of7M-16, McH1-7 or FSW (control) over time.

Effectiveness of probiotic Of7M-16 at treating infected M. cavernosa colonies

Similarly, the ability of Of7M-16 to successfully treat *M. cavernosa* colonies in aquaria was investigated. A total of 6 genotypes of *M. cavernosa* were each split into 3 fragments and then treated with McH1-7, Of7M-16 or FSW (control). All colonies were monitored and photographed over 21 days. The percentage of healthy tissue remaining over time was calculated (Fig. 7A) and subsequent AUC was compared between treatments (Fig. 7B; repeated measures ANOVA: $p = 0.086$, $n = 6$). A log-rank (Mantel-Cox) test compared the probability of survival between treatments over time (Fig. 8; $p = 0.385$, $n = 6$). Disease slowed on 2 out of 6 fragments treated with Of7M-16 and slowed or stopped on 4 out of 6 fragments treated with McH1-7 compared to controls. Of7M-16 performed no better on *M. cavernosa* than untreated controls. Initial results suggest that Of7M-16 may not be a successful treatment for *M. cavernosa* colonies, although differences between treatments were not significant.

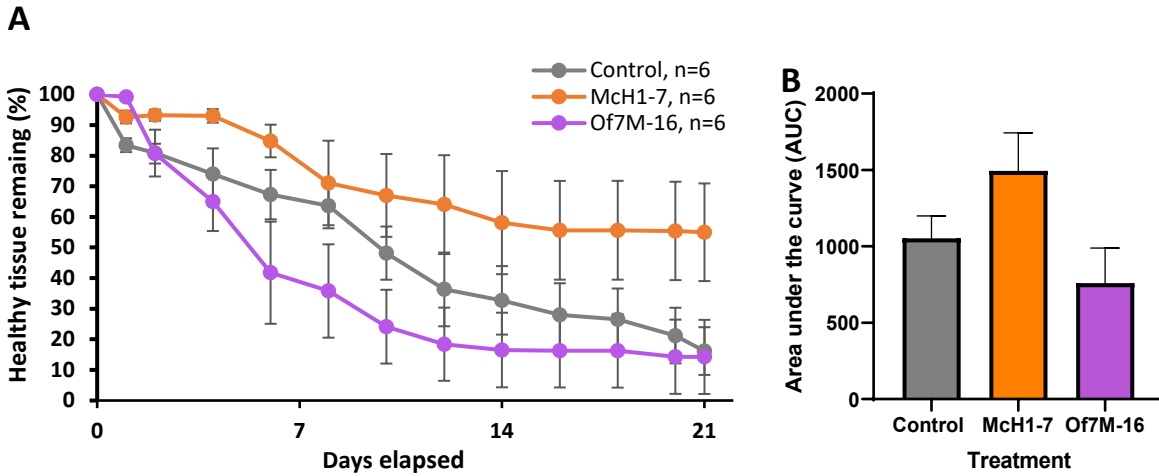


Figure 7. A) Percentage (mean \pm SE) of healthy tissue remaining on infected *M. cavernosa* fragments treated with Of7M-16, McH1-7 or FSW (control) and B) subsequent AUC with a larger AUC corresponding to slower disease progression. Data are shown as mean \pm 1 SEM.

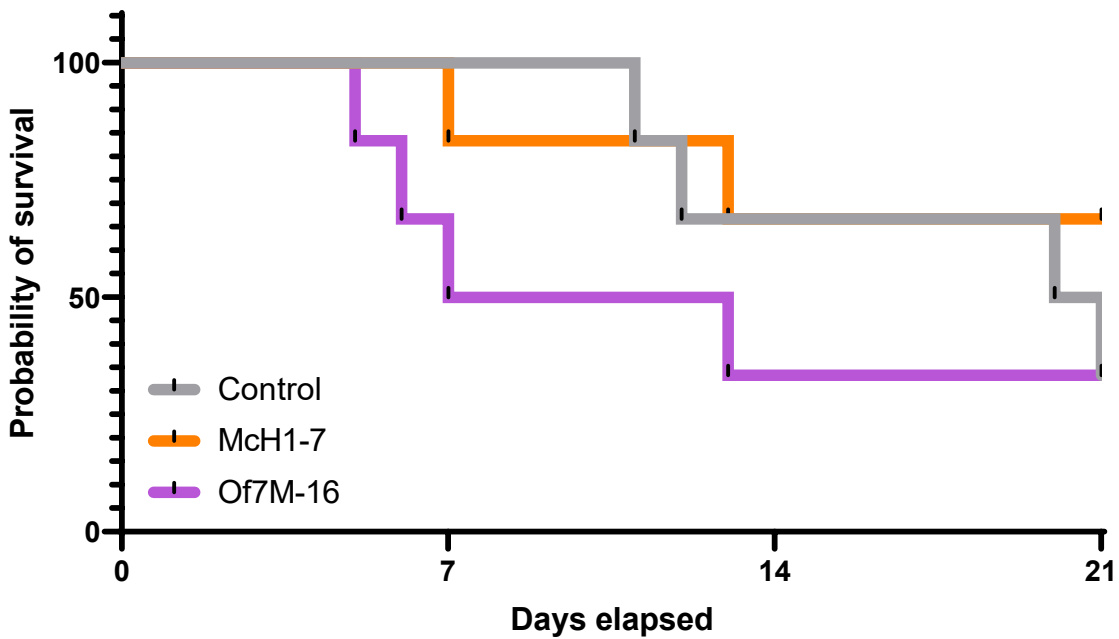


Figure 8. Kaplan–Meier survival analysis of the probability of survival of diseased *M. cavernosa* fragments of the same genotype treated with Of7M-16, McH1-7 or FSW (control) over time.

From these experiments, it was concluded that Of7M-16 is not a probiotic treatment worth pursuing in the future. Conversely, McH1-7 was successful at treating *M. cavernosa* and showed

similar effectiveness as Of7M-16 at treating infected *O. faveolata* colonies. McH1-7 is therefore the first treatment selected for further testing in the field.

To test combinational treatments of different probiotic strains on a wider variety of disease coral species.

Combinational probiotic treatments

Creating a mix of probiotics for coral treatments against SCTLD may reduce the chances of the pathogen(s) evolving resistance and potentially increase the efficacy of probiotic McH1-7. Potential synergistic effects of probiotic combinations were investigated by mixing two strains of probiotics immediately prior to spotting them onto plate assays with potential pathogens and determining the resulting zone of inhibition. Potential pathogens McT4-15, McT4-56, and OfT6-21 isolated from SCTLD lesions were used in this study. Multiple combinations of McH1-7 with other probiotics were able to inhibit the putative pathogens more than McH1-7 alone (Fig. 9).

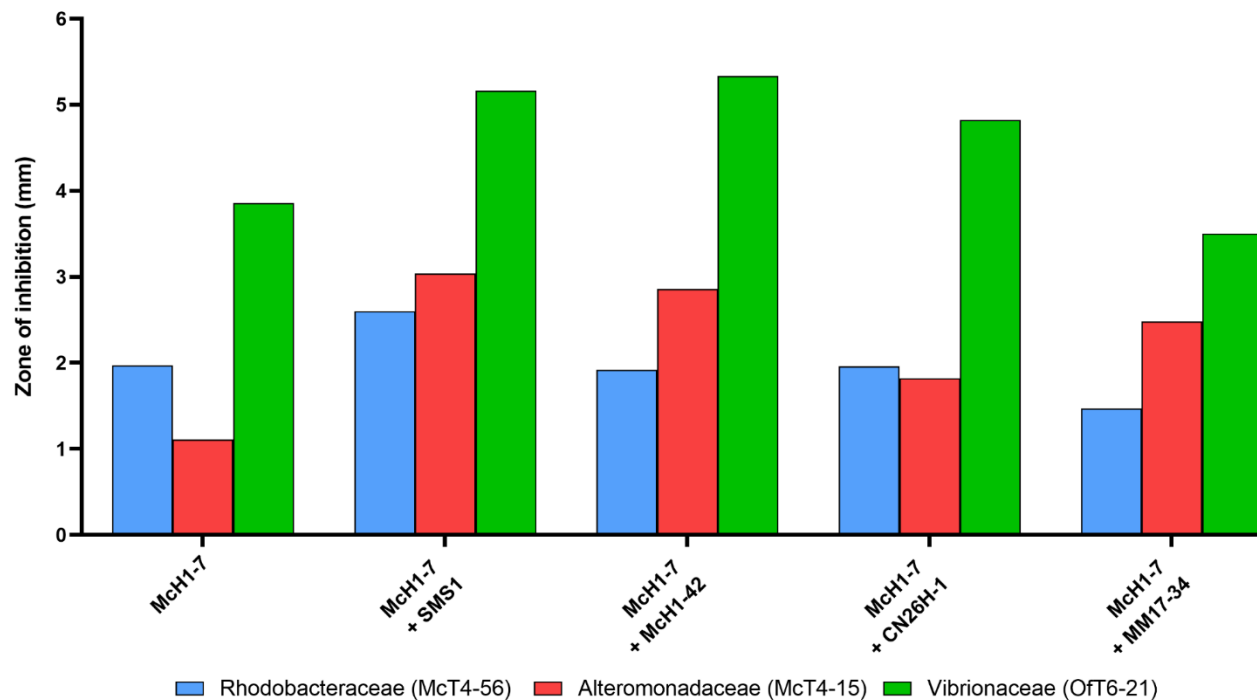


Figure 9. Zone of inhibition resulting from well plating combinational probiotics against three families of putative pathogens Rhodobacteraceae (blue), Alteromonadaceae (red), and Vibrionaceae (green).

The two mixes that created the largest zones of inhibition were mixtures of McH1-7 with strains SMS1 or McH1-42. These two mixtures were each separately tested on diseased *M. cavernosa*

colonies in laboratory aquaria. One fragment was inoculated with both McH1-7 and McH1-42. This treatment slowed the progression of the disease compared to the control treated with FSW over 21 days of experimentation. However, this fragment progressed faster than the fragment of the same genotype that was treated with McH1-7 alone (Fig. 10).

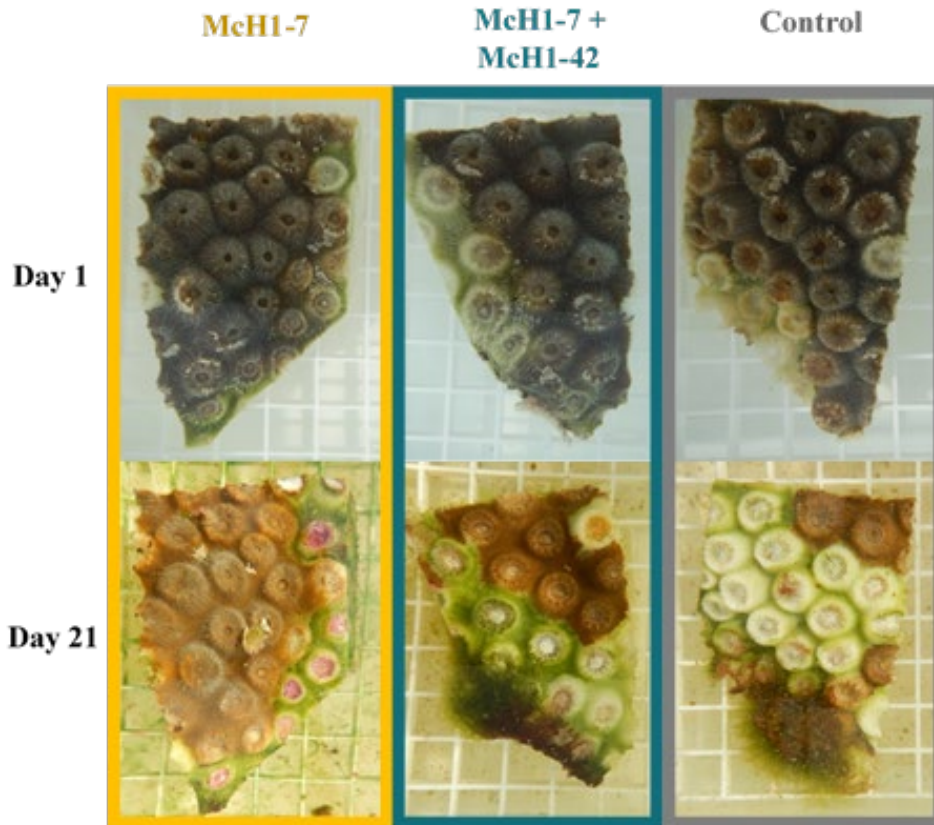


Figure 10. Progression of SCTLD over 21 days on fragments treated with McH1-7 or McH1-7 + McH1-42 compared to the control of the same genotype.

In addition, 6 genotypes of *M. cavernosa* were each split into 3 fragments to be treated with McH1-7, McH1-7 + SMS1, or FSW (control). All colonies were monitored and photographed over 21 days. The percentage of healthy tissue remaining over time was calculated (Fig. 11A) and subsequent AUC was compared between treatments (Fig. 11B; repeated measures ANOVA: $p = 0.406$, $n = 6$). A survival log-rank (Mantel-Cox) test compared the probability of survival between treatments over time (Fig. 12; $p = 0.638$, $n = 6$). Disease progression was slower on 5 of the 6 fragments compared to the controls. However, 50% of the fragments completely succumbed to the disease within 21 days. It has been concluded that McH1-7 alone is the most effective probiotic treatment for *M. cavernosa* compared to all other treatments tested.

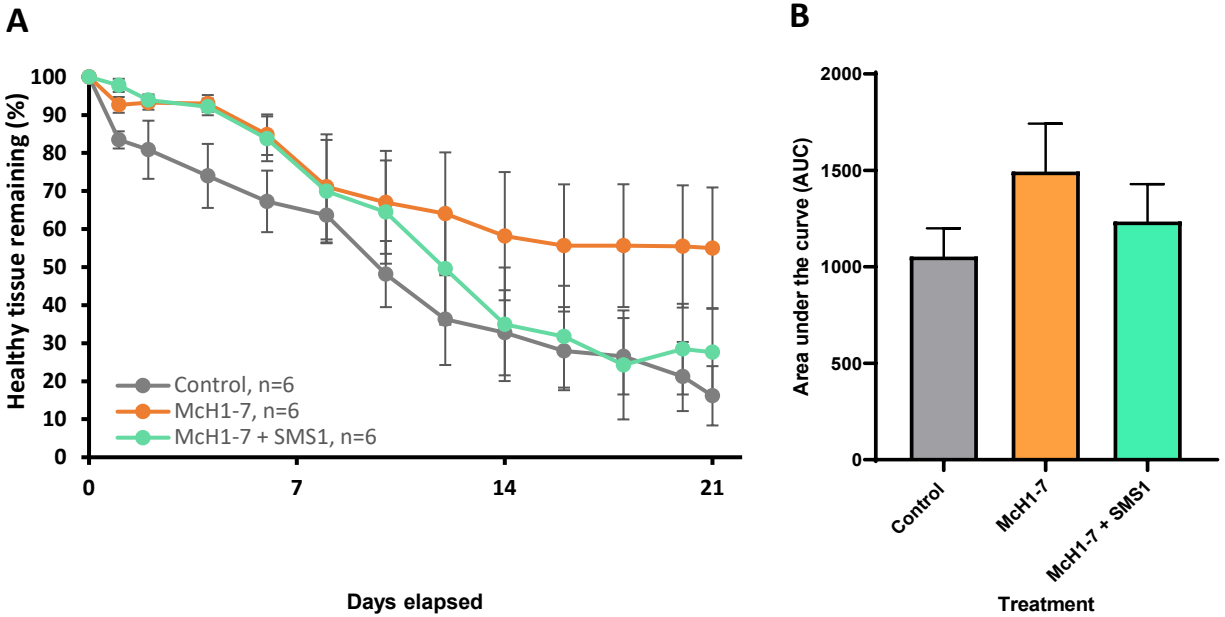


Figure 11. A) Percentage (mean \pm SE) of healthy tissue remaining on infected *M. cavernosa* fragments treated with McH1-7, McH1-7 + SMS1, or FSW (control) and B) subsequent AUC with a larger AUC corresponding to slower disease progression. Data are shown as mean \pm 1SEM.

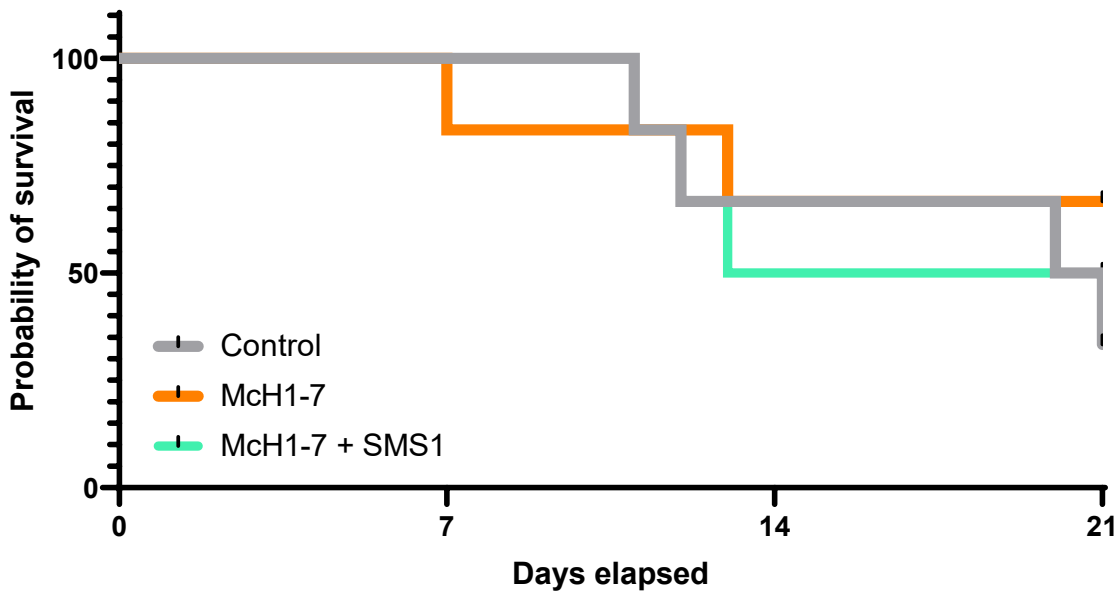


Figure 12. Kaplan-Meier survival analysis of the probability of survival of diseased *M. cavernosa* fragments of the same genotype treated with McH1-7, McH1-7 + SMS1, or FSW (control) over time.

Safety of probiotic McH1-7 with different coral species

As probiotic McH1-7 proved to be more effective than Of7M-16 or other combinational probiotic treatments, an experiment testing the safety of this probiotic on other coral species was conducted. McH1-7 was inoculated onto healthy fragments of *Colpophyllia natans*, *Siderastrea siderea*, *Stephanocoenia intersepta*, and *Meandrina meandrites* (n=2 coral fragments per species) and monitored over 21 days. McH1-7 did not visibly affect these species during the experiment (Fig. 13).

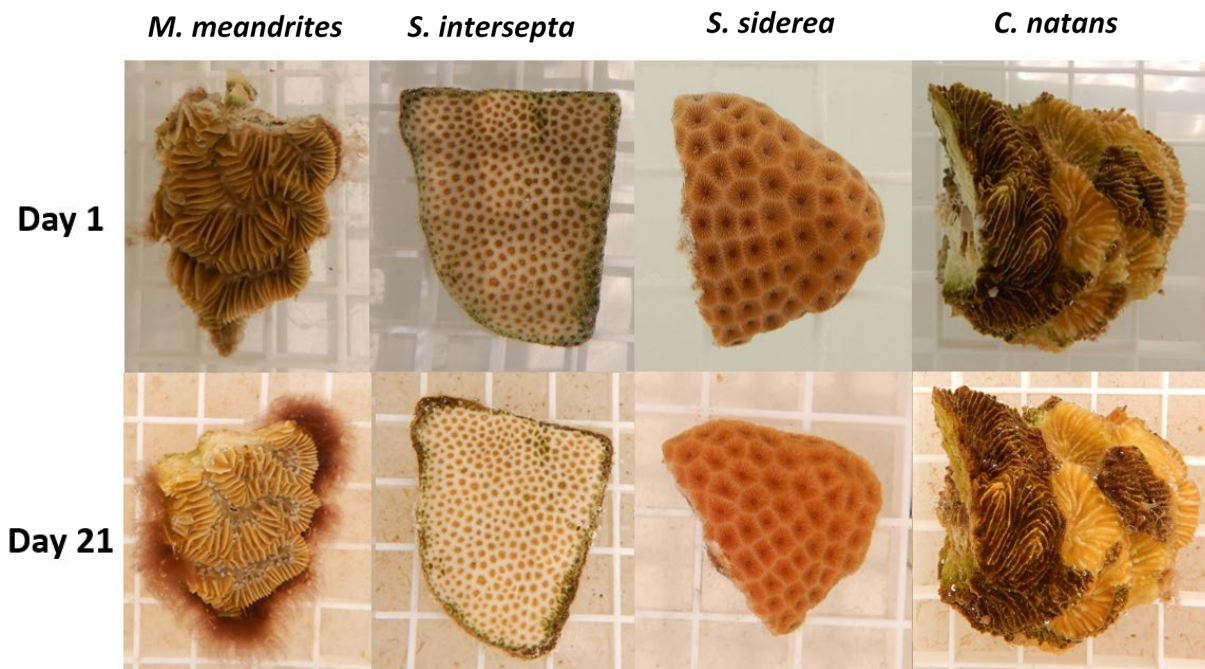


Figure 13. Examples of four species of coral each inoculated with McH1-7 and monitored over 21 days.

As McH1-7 did not produce any visible signs of stress from *C. natans*, an important reef building species, the effectiveness of McH1-7 to treat this species was investigated. Six different genotypes were each split into two fragments to be treated with either McH1-7 or FSW (control). All colonies were monitored and photographed daily. The percentage of healthy tissue remaining over time was calculated (Fig. 14A) and subsequent AUC was compared between treatments (Fig. 14B; paired t-test: $p = 0.0117$, $n = 6$). A survival log-rank (Mantel-Cox) test compared the probability of survival between treatments over time (Fig. 15; $p = 0.0027$, $n = 6$). Disease progression was significantly slower on fragments treated with McH1-7; however, all fragments died within 8 days of treatment. McH1-7 was not an effective treatment for *C. natans* to stop SCTL. However, it was able to significantly slow disease progression, suggesting the potential for probiotic treatments for *C. natans*.

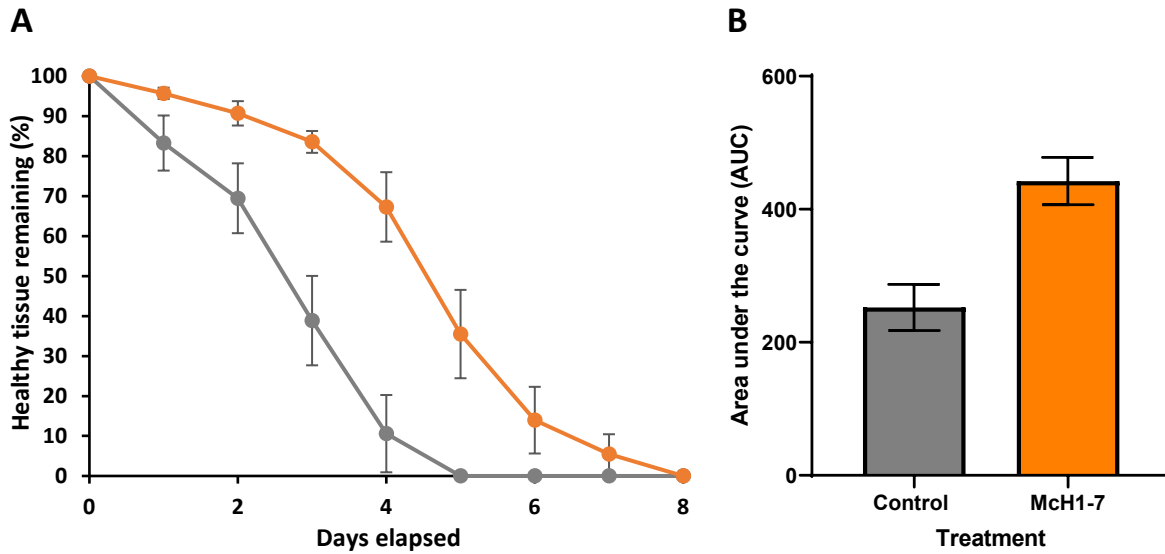


Figure 14. A) Percentage (mean \pm SE) of healthy tissue remaining on infected *C. natans* fragments treated with McH1-7 or FSW (control) and B) subsequent AUC with a larger AUC corresponding to slower disease progression. Data are shown as mean \pm 1SEM.

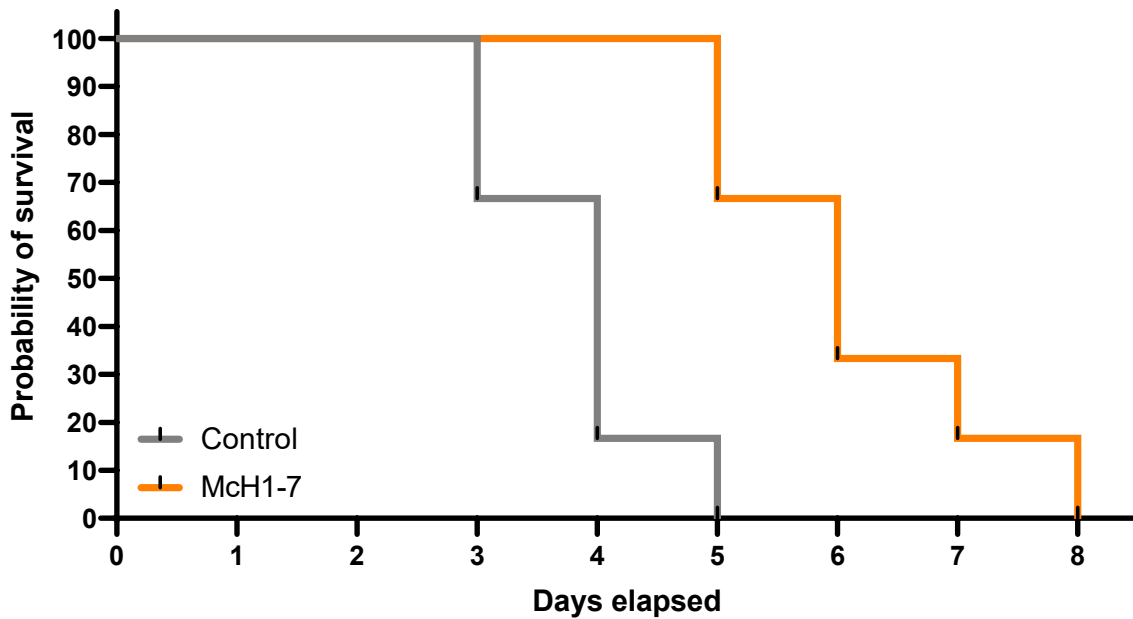


Figure 15. Kaplan–Meier survival analysis of the probability of survival of diseased *C. natans* fragments of the same genotype treated with McH1-7 or FSW (control) over time.

The effectiveness of probiotic McH1-7 was also tested on *Pseudodiploria strigosa* colonies infected with SCTLD. Two different genotypes were each split into two fragments to be treated

with either McH1-7 or FSW (control). All colonies were monitored and photographed over time. However, all four fragments succumbed to disease within five days of treatment (Fig. 16). McH1-7 is no longer being pursued as a viable treatment for *P. strigosa*.

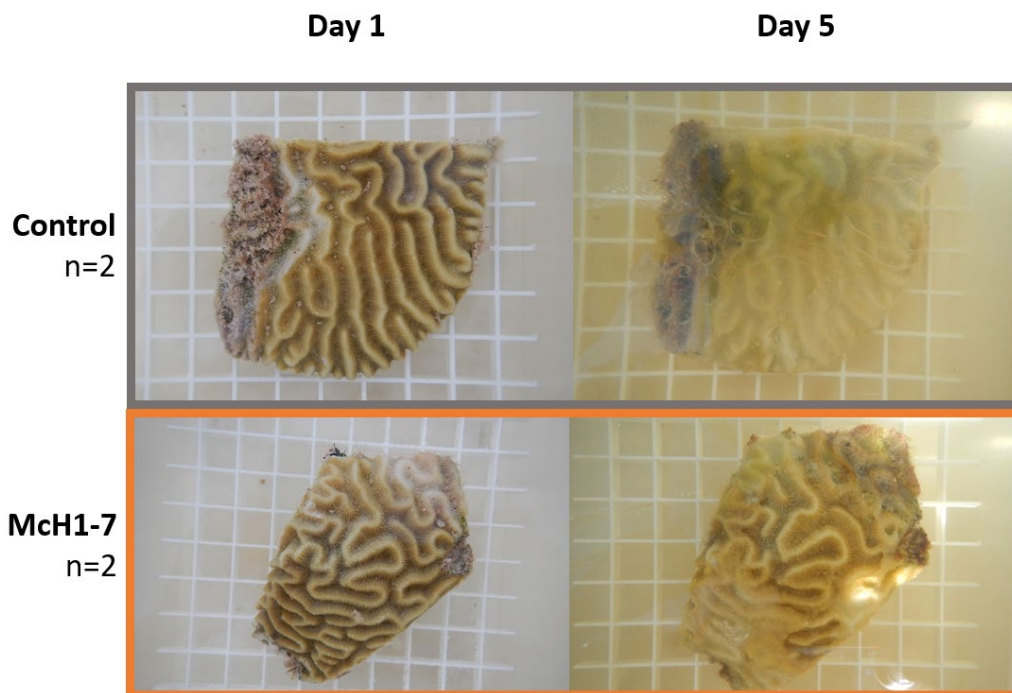


Figure 16. *P. strigosa* treated with McH1-7 or FSW (control) and monitored over time.

To characterize effective probiotics with complete genome sequencing and chemical analysis before potential deployment in the field.

To date, 66 isolates have been further pursued as promising candidates for probiotic development based on demonstrated inhibitory activity against at least one of the target strains (*Leisingera sp.* McT4-56, *Alteromonas sp.* McT5-15, *Vibrio coralliilyticus* OfT6-21). All of these strains have been tested for the presence of bioactive small molecules. For 25 strains (38%) we were unable to replicate the inhibitory activity of the live cells with their organic extracts, indicating the presence of antimicrobial properties that are not extractable using organic solvent methods. We can conclude that these strains are not likely making small molecule antibiotics, or the compounds are unstable, but are more likely producing enzymes or physical defenses that are the basis of their antimicrobial properties. Of the remaining 41 strains, 18 produced fatty acid glycosides and 11 produced fatty acids with phosphoethanolamine groups that demonstrated antibacterial activity. Two strains, McH1-7 and Of7-M16, produced specific small molecules that have been completely characterized. McH1-7 produces the compounds korormicin A and tetrabromopyrrole. Based on the complete genome sequence of this strain, we know that it also has the genes to produce other classes of compounds including marinocine. The second strain, Of7-M16, produces the known antibiotic compounds violacein, thiomarinols A and B and additional fatty acid phosphoethanolamines. Finally, the remaining ten strains are currently in the

process of being chemically characterized. Organic extracts of these strains are active against at least one of the target strains (putative pathogens). We continue to screen strains for activity and move promising strains into the pipeline for chemical characterization and genomics.

Representative candidates in our pipeline include the following (Table 1), with an emphasis on those from *C. natans* and *M. meandrites* as well as new strains from *O. faveolata* next year.

Table 1. Representative probiotic strains in the pipeline for probiotic development.

Strain	Description	Closest match with 16S rRNA gene	Morphology	Isolated from?
McH1-25	Inhibitory isolate from a disease resistant <i>M. cavernosa</i> .	Not done	purple	<i>M. cavernosa</i>
CN68H-1	Inhibitory isolate from a healthy <i>C. natans</i> .	Not done	cream, translucent	<i>C. natans</i>
CNMC5-1	Inhibitory isolate from a disease-resistant <i>M. cavernosa</i> genotype from disease <i>M. meandrina</i> transmission.	Not done	pink, opaque	<i>M. cavernosa</i>
CNMC7-37	Inhibitory isolate from a disease-resistant <i>M. cavernosa</i> genotype from disease <i>M. meandrina</i> transmission.	Not done	grey-cream, opaque	<i>M. cavernosa</i>
McH1-61	Inhibitory isolate from a disease resistant <i>M. cavernosa</i> .	Not done	white	<i>M. cavernosa</i>
DSH1-31	Inhibitory isolate from a disease resistant <i>D. stokesii</i> .	Not done	N/A	<i>D. stokesii</i>
MMH1-48	Inhibitory isolate from a disease resistant <i>M. meandrina</i> .	Not done	purple	<i>M. meandrites</i>
MM17-29	Inhibitory isolate from a disease resistant <i>M. meandrites</i> .	Not done	yellow, translucent	<i>M. meandrites</i>
CNC9-20	Inhibitory isolate from a disease resistant <i>M. meandrites</i> .	Not done	pink, opaque	<i>M. meandrites</i>
CnH1-48	Healthy <i>C. natans</i> , isolate appears to produce a bactericidal compound effective against all target strains.	Not done	neon green	<i>C. natans</i>
MMH1-66	Inhibitory isolate with broad-spectrum activity, but extracts were inactive. Had strongest antibacterial activity against <i>V. coralliilyticus</i> .	<i>Pseudoalteromonas phenolica</i>	N/A	<i>M. meandrites</i>
MM17-31	Inhibitory isolate with strong specific activity against Vibrios. Produces inhibitory fatty acid glycosides.	<i>Psychrobium conchae</i>	White, opaque	<i>M. meandrites</i>
MM17-34	Inhibitory isolate with activity against <i>V. coralliilyticus</i> . Chemistry incomplete.	<i>Halomonas</i> sp.	Cream, opaque	<i>M. meandrites</i>
MCA-3	Inhibitory isolate with specific activity against Vibrios. Extracts are inactive.	<i>Bacteroidetes</i> sp.	Peach, opaque	<i>M. cavernosa</i>
DSH1-27	Inhibitory isolate from a disease resistant <i>D. stokesii</i> .	Not done	N/A	<i>D. stokesii</i>

Task 3: To test alternative treatments and diagnostic tools to complement probiotic treatments.

To continue testing the effects of essential oils (or other antibacterials) as an alternative treatment of SCTL D lesions or if they can supplement the probiotic treatments.

Essential oils have been used in aquaculture for their antimicrobial properties. They represent a more-affordable, non-antibiotic alternative treatment for SCTL D. The goal is that these oils inhibit putative pathogens of SCTL D while allowing for the growth of probiotic bacteria so that they could be used in conjunction with probiotic treatments. To investigate essential oils that may exhibit both qualities, probiotics Mch1-7 and SMS-1 were assayed against a variety of essential oils by well diffusion. After 24 h, the radius of the zone of inhibition was measured from the inner edge to the outer edge of the zone of inhibition (Fig. 17). Essential oils with the smallest zones of inhibition that showed they did not inhibit growth of the probiotics were considered most promising for use as a treatment against SCTL D.

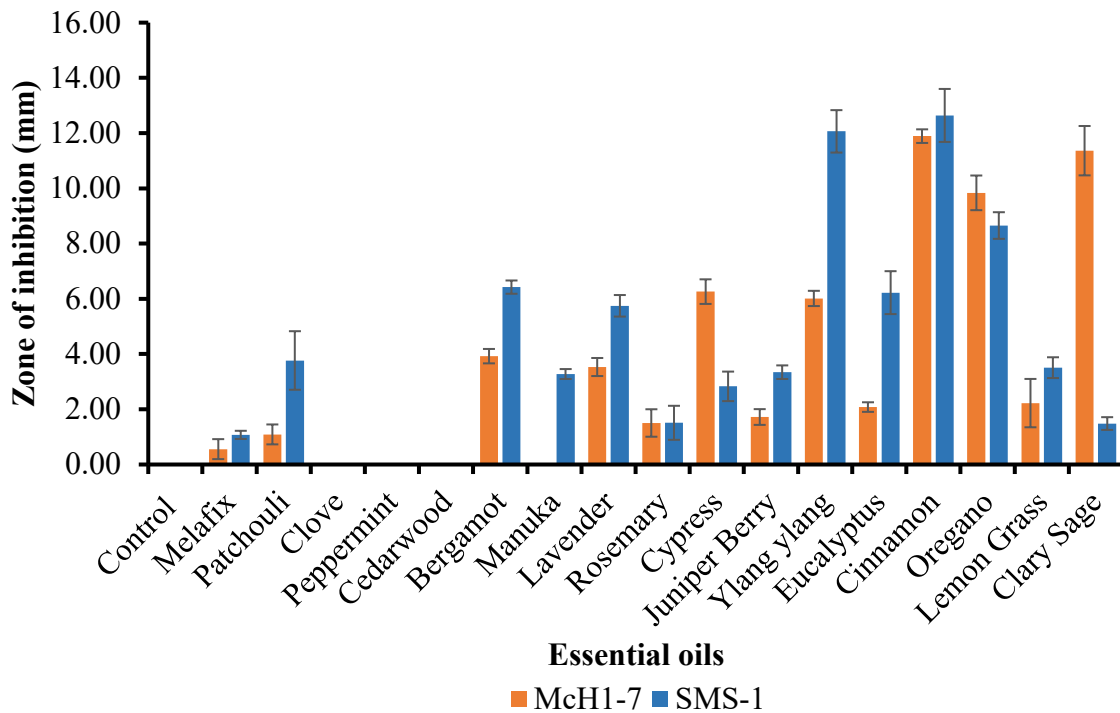


Figure 17. Length of the zone of inhibition resulting from assays of both Mch1-7 and SMS-1 against a variety of essential oils. Data are shown as mean and SEM ($n=3$ for each treatment).

In addition, putative pathogens were then assayed against essential oils by well diffusion. After 24 h, the radius of the zone of inhibition was measured from the inner edge to the outer edge of the zone of inhibition. Essential oils with the largest zones of inhibition were considered most promising for use as a treatment against SCTL D. Oregano, lemon grass, and clary sage were more effective at inhibiting the growth of putative pathogens (Fig. 18).

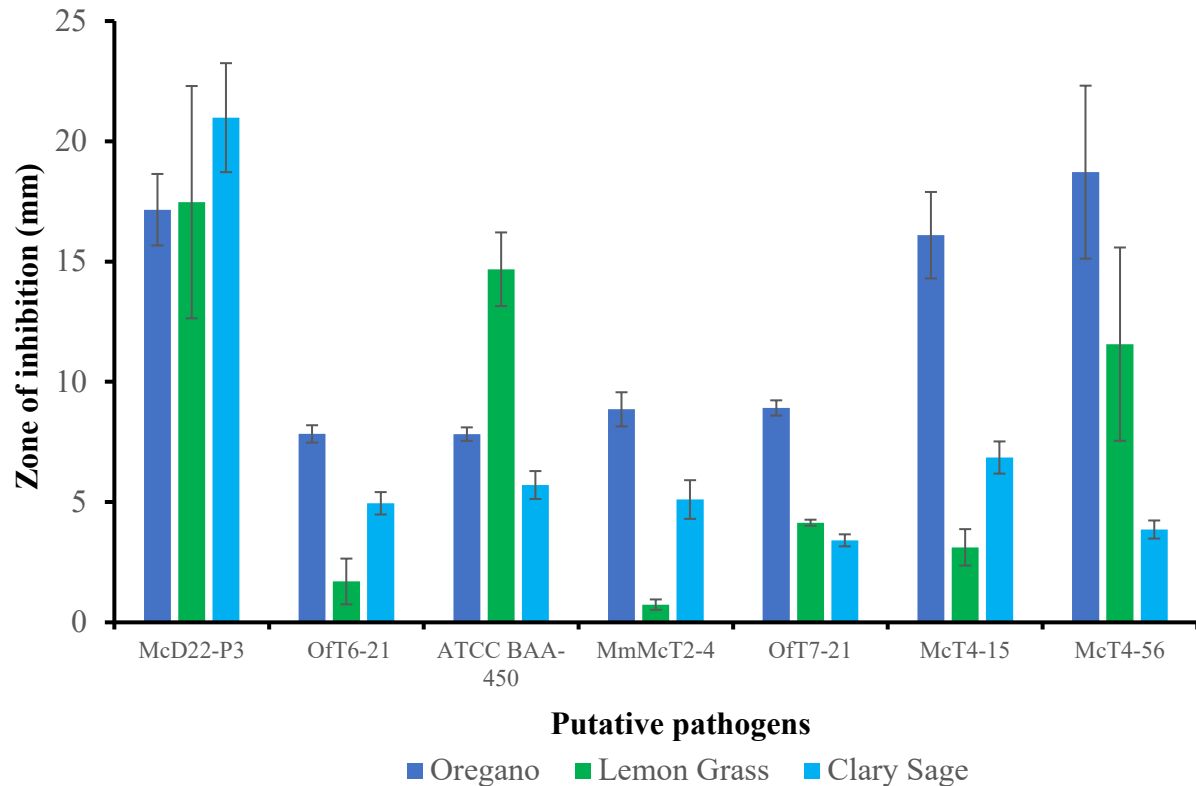


Figure 18. Size of the zones of inhibition resulting from assays of 7 putative pathogens against three different essential oils. Data are shown as mean and SEM ($n=3$ for each treatment).

Oregano, lemon grass, and clary sage were tested on 5 diseased *O. faveolata* fragments from 4 different genotypes that were infected with SCTLD. The two fragments that came from the same genotype were cut from two different lesions on the colony. All fragments were simultaneously dipped in a 5 L tank of FSW containing 1:1000 dilution of each essential oil for 30 mins. The tank contained an airline to provide oxygen to the fragments and aid in mixing. Four fragments had died within three days of treatment, comparatively faster than the control corals (Table 2), suggesting that essential oils may have caused harm to the corals. Essential oils are no longer being pursued by us as a treatment for SCTLD.

Table 2. Disease outcomes over 21 days for fragments treated with essential oils in the laboratory.

Coral Colony ID	Control	Fragment 1	Fragment 2
OfD-24	Disease not progressing	Disease not progressing	N/D
OfD-25	Complete mortality day 7	Complete mortality day 2	Complete mortality day 2
OfD-26	Complete mortality day 3	Complete mortality day 2	N/D
OfD-29	Complete mortality day 17	Complete mortality day 3	N/D

To continue screening diseased corals using the immunological assays specific to *V. coralliilyticus* to assess the potential threat posed by the pathogen and interference with probiotic treatment.

Examination of the role of *Vibrio coralliilyticus* in SCTLD infections was conducted from 2018-2020. The presence of this bacterium was associated with faster disease progression and higher mortality rates, regardless of the location of the coral along the FRT. These results suggest that *V. coralliilyticus* may be causing a coinfection on these corals. To continue the investigation of the role of *V. coralliilyticus* in SCTLD infections, all diseased corals collected for experiments were screened with an immunoassay specific to a toxic protein produced by this bacterium. The *Vibriosis VcpA RapidTest* (mAbDx, Inc.) was created to detect the toxic metalloprotease, VcpA, produced by pathogenic strains of *V. coralliilyticus* that can degrade living tissue. The test has been incorporated into robust single-use cassettes suitable for both the laboratory and field settings (Fig. 19).

A total of 102 corals have been screened for VcpA by this method, 19 of which were positive (18.6%). This includes 16 out of 67 *M. cavernosa* colonies (23.8%), and 5 out of 24 *O. faveolata* colonies (20.8%). The rest of the colonies tested included *P. strigosa* and *C. natans*, none of which were positive for VcpA.

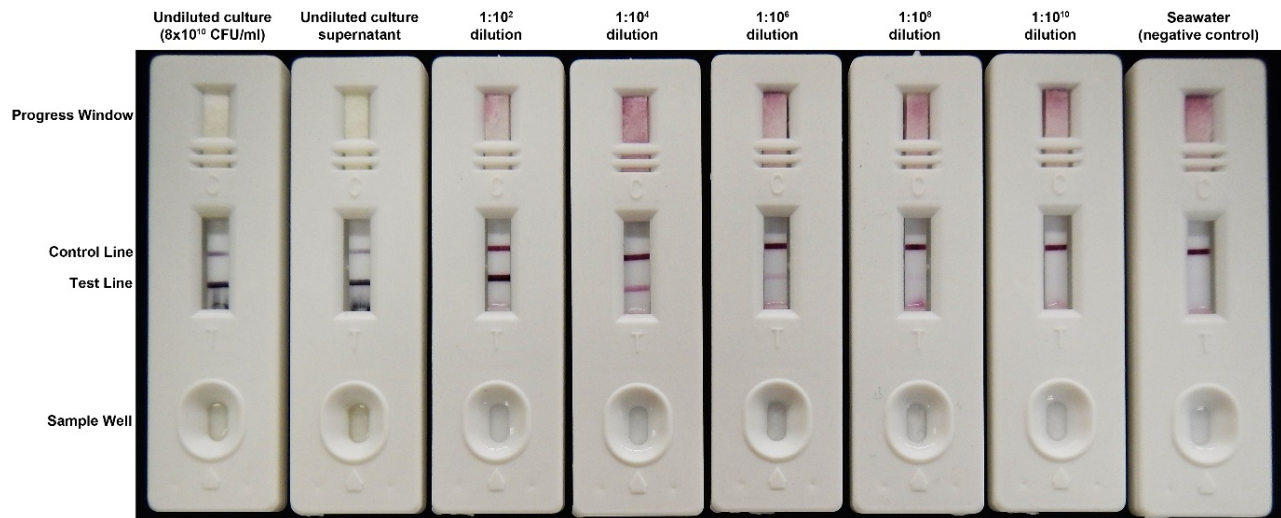


Figure 19. *Vibriosis VcpA RapidTest* cassettes displaying a positive (left) and a negative (right) sample for VcpA. The coral sample is slowly added into the sample well until it reaches the progress window via capillary action. A clear two-line result indicates a sample positive for VcpA whereas a single line indicates a negative result.

The results from the *Vibriosis VcpA RapidTests* were analyzed in a variety of ways to better understand the progression of disease and the mortality rate associated with the presence of *V. coralliilyticus*. The progression rate of *M. cavernosa* lesions in the presence of *V. coralliilyticus* was compared by conducting a two-tailed Wilcoxon test on the AUC (Fig. 20; $n = 67$, $p < 0.0001$). As a smaller AUC suggests the lesions are progressing faster, corals positive for VcpA had significantly more aggressive lesions.

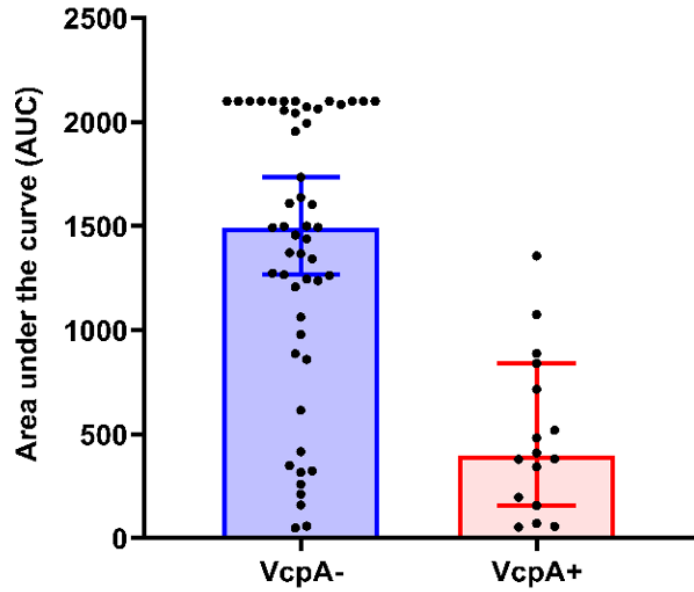


Figure 20. Area under the curve (AUC) analysis for VcpA⁻ (blue, n = 51) and VcpA⁺ (red, n = 16) diseased *M. cavernosa* with a smaller AUC corresponding to faster disease progression. Data shown are median and 90% confidence intervals (CI).

Likewise, the mortality rate of infected *M. cavernosa* in the presence of *V. coralliilyticus* was compared by a Mantel-Cox test (Fig. 21; $n = 67, p < 0.0001$). The mean survival of infected *M. cavernosa* that were negative for VcpA was 17.4 d, whereas the mean survival for fragments positive for VcpA was greatly reduced to 8.5 d (Fig. 21, Fig. 22).

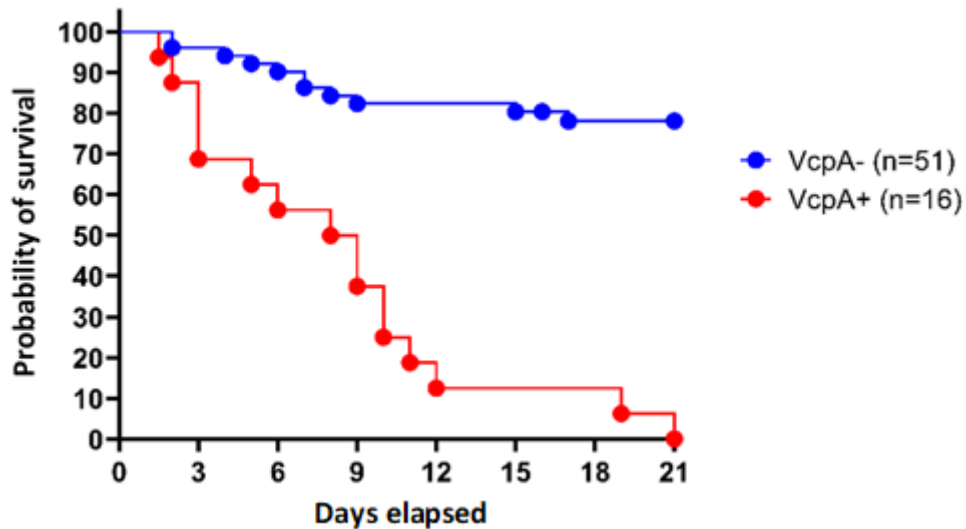


Figure 21. Kaplan-Meier survival curves of diseased *M. cavernosa* colonies negative for VcpA (blue lines) and positive for VcpA (red lines).

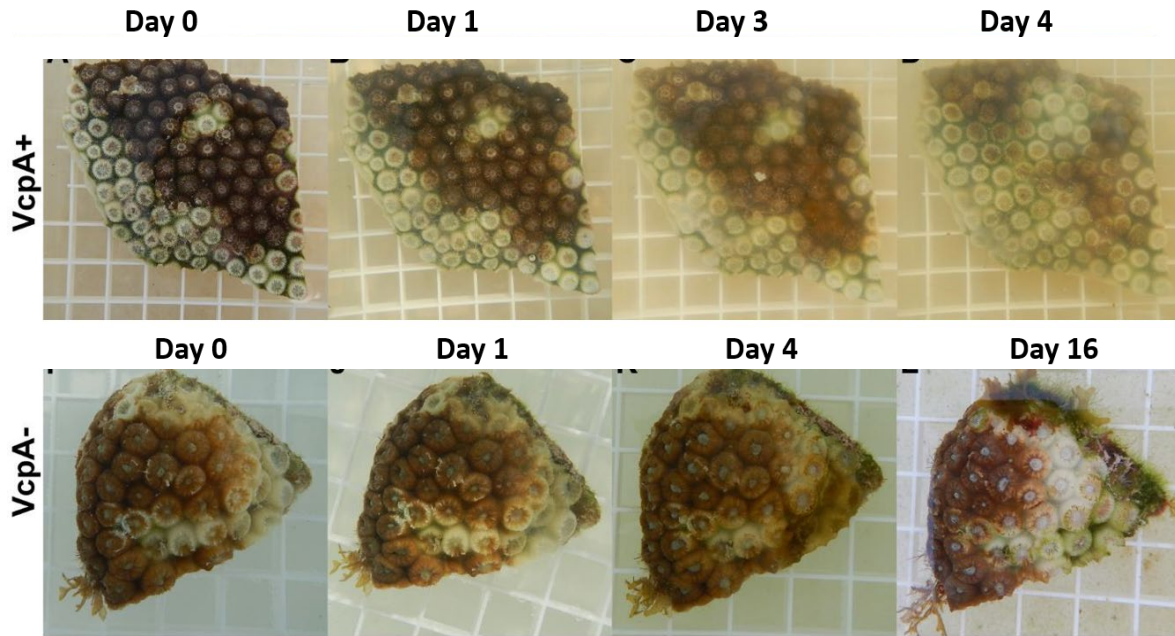


Figure 22. Example of the faster mortality rate seen in infected *M. cavernosa* colonies positive for VcpA (top fragment) versus negative for VcpA (bottom fragment). Note different time scales for the VcpA positive and VcpA negative rows.

Results from the *Vibriosis VcpA RapidTests* for *O. faveolata* were also analyzed to determine if the presence of *V. coralliilyticus* increases lesion progression and rate of mortality of infected *O. faveolata*. The progression rate of *O. faveolata* lesions in the presence of *V. coralliilyticus* was compared by conducting a two-tailed Wilcoxon test on the AUC (Fig. 23; $n = 24$, $p = 0.0058$). As a smaller AUC suggests the lesions are progressing faster, corals positive for VcpA had significantly more aggressive lesions.

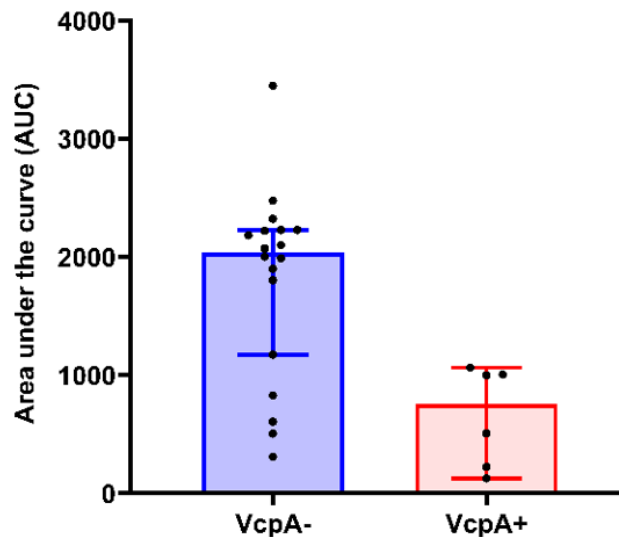


Figure 23. Area under the curve (AUC) analysis for VcpA⁻ (blue, $n = 18$) and VcpA⁺ (red, $n = 6$) diseased *O. faveolata* with a smaller AUC corresponding to faster disease progression. Data shown are median and 90% CI.

The mortality rate of infected *O. faveolata* in the presence of *V. coralliilyticus* was compared by conducting a Mantel-Cox test (Fig. 24; $n = 24$, $p = 0.002$). The mean survival of infected *O. faveolata* that were negative for VcpA was 17.8 d, whereas the mean survival for fragments positive for VcpA was reduced to 10.5 d.

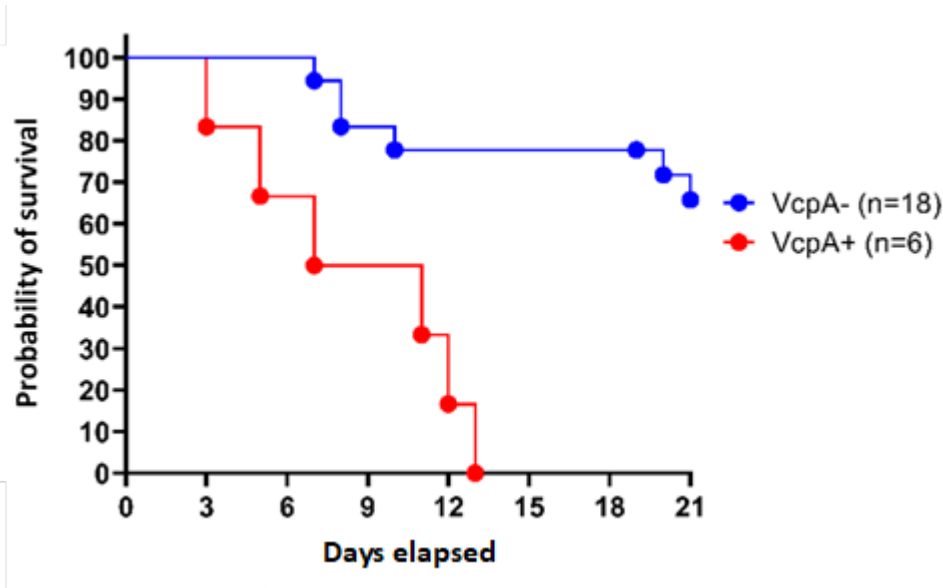


Figure 24. Kaplan-Meier survival curves of diseased *O. faveolata* colonies negative for VcpA (blue lines) and positive for VcpA (red lines).

These results suggest that *V. coralliilyticus* has an alarming effect on lesion progression and mortality rates of both diseased *M. cavernosa* and *O. faveolata*. *V. coralliilyticus* is not found on all diseased corals, suggesting this bacterium is not the main cause of SCTLD, but instead could escalate chronic or sub-acute lesions to acute lesions as a coinfection (Fig. 25).

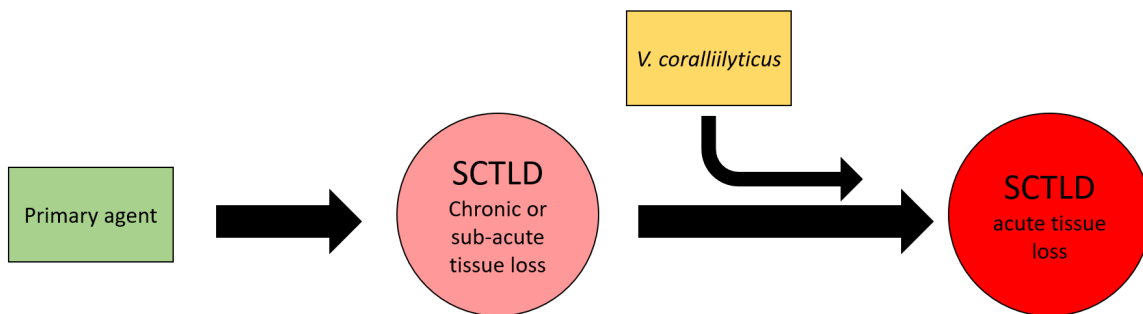


Figure 25. Example of how a primary agent of SCTLD causes chronic or sub-acute tissue loss before a coinfection of *V. coralliilyticus* causes acute tissue loss.

It is important to understand if this bacterium has more of an impact at specific locations along the Florida Reef Tract. Therefore, *M. cavernosa* collected from Broward County and the FL Keys were compared to determine if progression rates associated with *V. coralliilyticus* vary by location (Fig. 26). There was no significant difference in AUC values between corals located in the Florida Keys or Ft. Lauderdale that were negative for *V. coralliilyticus* (Tukey's, $p = 0.57$). Likewise, there was no significant difference between corals located in the Florida Keys or Ft. Lauderdale that were positive for *V. coralliilyticus* (Tukey's, $p = 0.88$). These results suggest that the progression rate is dependent on the presence of *V. coralliilyticus* and not location along the FRT.

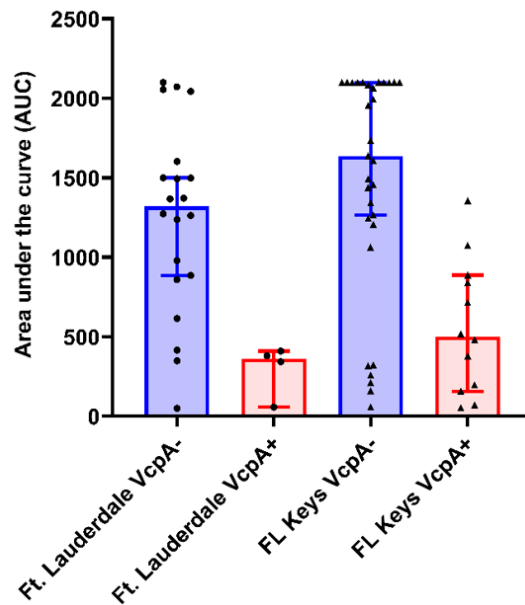


Figure 26. AUC comparison of diseased *M. cavernosa* colonies negative for VcpA (blue) or positive for VcpA (red) and separated between the Florida Keys or Ft. Lauderdale locations. Data shown are median and 90% CI.

To determine if mortality rates of *M. cavernosa* positive for *V. coralliilyticus* vary by location, a comparison of the survival curves was conducted (Fig. 27). There was no significant difference in mortality rate between corals located in the Florida Keys or Ft. Lauderdale that were negative for *V. coralliilyticus* (Mantel-Cox; $p = 0.65$). Likewise, there was no significant difference between corals located in the Florida Keys or Ft. Lauderdale that were positive for *V. coralliilyticus* (Mantel-Cox; $p = 0.15$). These results suggest that the mortality rate is dependent on the presence of *V. coralliilyticus* and not location along the Florida reef tract.

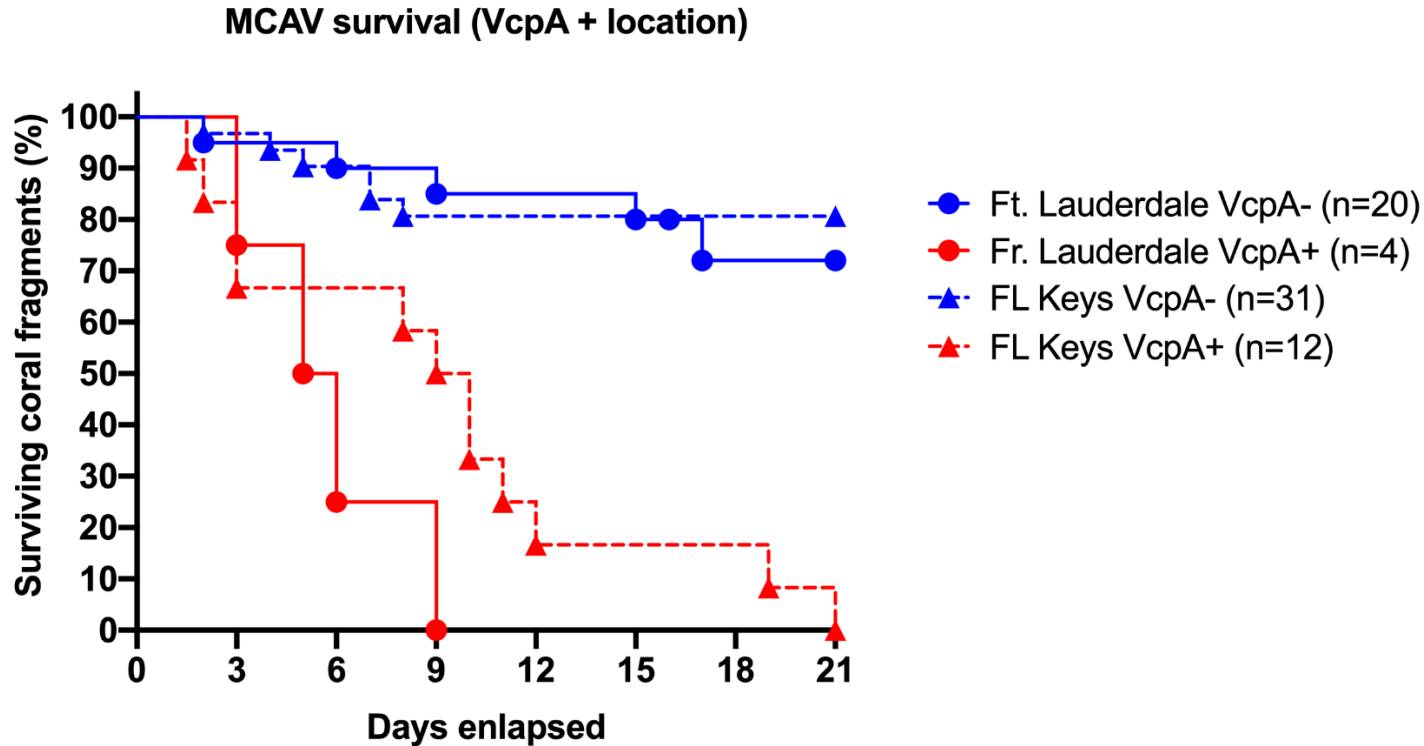


Figure 27. Kaplan-Meier survival curves of diseased *M. cavernosa* colonies negative for VcpA (blue lines) or positive for VcpA (red lines) and separated between the Florida Keys (dotted lines) or Ft. Lauderdale (solid lines) locations.

V. coralliilyticus as a species is known to be resistant to a variety of different antibiotics, making infections caused by this bacterium difficult to treat. Alarming, lesions positive for *V. coralliilyticus* were significantly harder to treat with McH1-7 (Fig. 28; log rank (Mantel-Cox) test: $p = 0.0075$, $n = 9$ pairs). We were able to get VcpA results with 18 colonies, with 50% (9 colonies) testing positive for VcpA. For the VcpA- colonies, 7 of 9 had arrested disease progression after treatment with McH1-7, in comparison to the VcpA+ colonies where only 2 of 9 had arrested disease progression. These results demonstrate how important it is to target probiotic treatments that are specifically more effective against and resistant to *V. coralliilyticus* in the future.

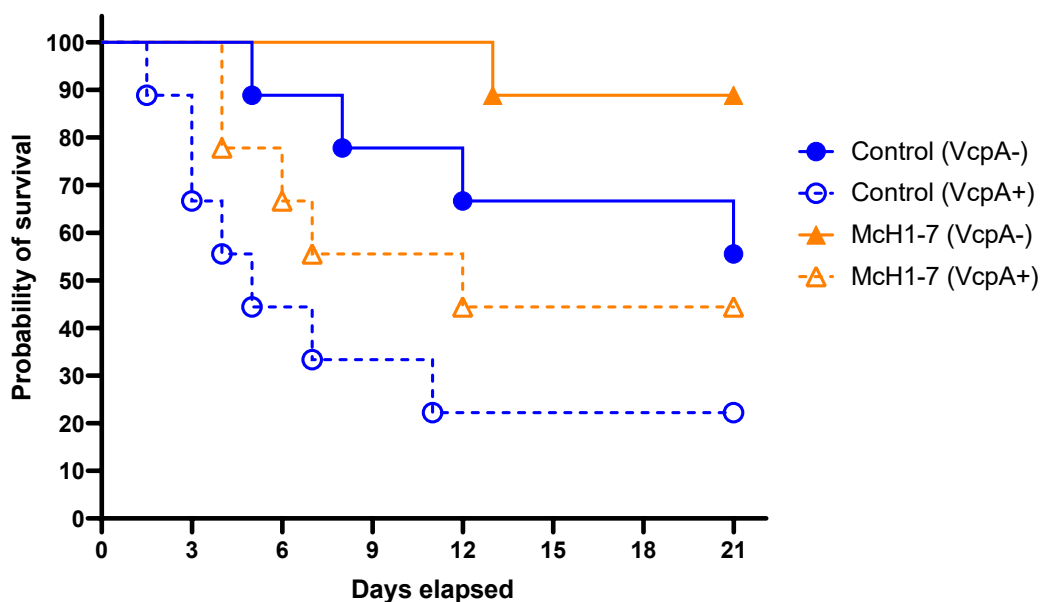


Figure 28. Survival curves of diseased *M. cavernosa* colonies negative for VcpA (solid lines) or positive for VcpA (dotted lines) and separated between McH1-7 (orange lines) or control (blue lines) treatments, $n=9$ for each treatment pair and VcpA reaction result.

To identify molecular markers for diseased colonies and indicators of treatment success using metabolomics for development of diagnostic tools to accompany disease treatments.

Dr. Neha Garg, School of Chemistry and Biochemistry, Georgia Institute of Technology has joined this project as a collaborator via a subaward to Georgia Tech to apply metabolomics methods to the study of SCTL. Metabolomics is an emerging technology that involves the comprehensive analysis of metabolites in a biological specimen through a combination of chemical extractions and analysis combined with bioinformatics to map out all the small molecule metabolites detectable in a sample. Metabolomics has been utilized for the first time in this project to characterize SCTL as well as the antibiotics and other metabolites present in the bacterial strains we are developing as probiotics. Healthy corals collected in January 2020 on the Dry Tortugas trip sponsored by FL-DEP were sampled for metabolomics to establish a baseline for Florida corals ahead of the disease front. Additionally, syringe samples of healthy and diseased coral tissue and mucus from Broward County that were treated with the probiotic McH1-7 on January 16, 2020 were also analyzed.

Analysis Workflow

The samples were analyzed using an Agilent 1290 Infinity II ultra-performance liquid chromatography (UPLC) system coupled to Bruker Impact II ultra-high resolution Qq-TOF mass spectrometer equipped with an ESI source and subjected to tandem mass spectrometry (MS/MS) analysis. A Kinetex 1.7 μm C18 reversed phase UPLC column (50 \times 2.1 mm) was employed for chromatographic separation. MS spectra were acquired in positive and negative ionization mode, m/z 50–2000 Da. An active exclusion of two spectra was employed, implying that an MS¹ ion would not be selected for fragmentation after two consecutive MS² spectra had been recorded for

it in a 0.5 min time window. For acquiring MS² data, eight most intense ions per MS¹ spectra were selected. The chromatography solvent A: water + 0.1% v/v formic acid and solvent B: MeCN + 0.1% v/v formic acid were employed. Flow rate was held constant at 0.5 mL/min throughout.

The LC-MS/MS data acquired above were analyzed using various strategies to annotate the metabolite features detected. First, molecular networks were generated based on MS² spectra. To aid structural annotations, the experimental MS² spectra are aligned with MS² spectra of known compounds. The MS² spectral libraries housed at the Global Natural Products Social Molecular Networking server (GNPS) include MS² spectra of compound collections from the FDA, NIH, third party spectral libraries, and user-submitted annotations. Second, the mzXML files were pre-processed using MZmine 2, an open source software. The output file is submitted to GNPS for Feature Based Molecular Networking (FBMN), along with a metadata file. The feature table output with relative abundances of each ion was also utilized to build statistical models and to rank metabolite features that distinguish healthy samples from diseased samples.

When GNPS cannot offer putative identifications, a variety of in-silico tools are used to predict compound identifications. For example, features can be submitted to the SIRIUS platform. SIRIUS is open source software that uses information contained in a feature's MS¹ and MS² spectra and considers the isotopic peak pattern to propose a chemical formula. A feature's fragmentation from MS/MS can be analyzed through SIRIUS by generating a fragmentation tree. Each fragment is given a potential molecular formula. The next step includes uploading the fragmentation tree to CSI:FingerID, which searches several biological and non-biological databases to suggest known compounds that fit both the proposed molecular formula by SIRIUS and the fragmentation tree. The CSI:FingerID output also ranks the likelihood the substructures of each proposed molecule can be explained by the fragments in the MS² spectra. CANOPUS, a recent addition to the SIRIUS platform, takes the compounds proposed by CSI:FingerID and suggests a molecular class to which the feature may belong. Thus, submitting a feature's MS¹ and MS² files to the SIRIUS platform results in a proposed molecular formula, potential known compounds, and a likely chemical classification. The SIRIUS outputs are cross-referenced with other molecular databases and published literature searches.

Results

Analysis of bacterial extracts. The antibacterial activity of extracts from potential probiotic bacterial strains were determined against three putative pathogens Mc4-56 (a *Leisingera* sp.), McT4-15 (an *Alteromonas* sp.) and OfT6-21 (*Vibrio coralliilyticus*) using agar disk-diffusion assay by the laboratory of Dr. Valerie Paul. These extracts were further fractionated, and the antibacterial activity of each fraction was determined. These fractions were designated as either active or inactive based upon the development of zones of inhibition in the agar disk-diffusion assay. In silico methods were used to annotate compounds with high bioactivity scores using CSI:Finger ID (Fig. 3). Korormicin was detected in a McH1-7 extract that was freeze-dried and extracted using 2:2:1 methanol:ethyl acetate:water solvent as expected. Marine bacteria are known to produce this compound, which has specific antibacterial activity against Gram negative

halophilic and marine bacteria. Thiomarinol A was detected in SSOFC5-18 and CN68H-1. This feature clustered with a node with a similar m/z 641.256 with a Retention Time (RT) shift of about 19 seconds, suggesting one of these two nodes could be an isomer to thiomarinol A. This cluster also included a node identified as thiomarinol B. Xenorhabdins 1 and 3 were detected in active fractions of SSOFC5-18 and CN68H-1. Lastly, various additional features associated with antibacterial properties were not identified using libraries housed at GNPS. Thus, using our methodology, we can detect a diverse set of natural products as well as identify known microbial molecules. These methods provide the ability to speed up the search for novel strains of bacteria that can be developed as probiotics by quickly dereplicating bacterial strains that might be taxonomically similar and are producing similar compounds.

Metabolomic analysis of healthy corals collected from Dry Tortugas for validation of LC-MS/MS method. During January 28-29, 2020, two members of Dr. Paul's laboratory had the opportunity to participate in a short cruise sponsored by the Florida Department of Environmental Protection to the Dry Tortugas to collect coral samples ahead of the disease front. The purpose of this cruise was to collect corals that had not yet been exposed to SCTLD that could be used for multiple experiments. Permit FKNMS-2019-160 to Valerie Paul covered the collection of corals on this cruise. During the cruise, corals were maintained in the live wells on the boat, and they were in excellent condition at the end of the cruise. After the cruise, corals were transported back to the Smithsonian Marine Station where they were placed in aerated buckets of filtered seawater and maintained for 5 days to allow them time to recover after transport. On February 4, the corals were cut into smaller pieces with a rock saw for various experiments. The saw blade was constantly sprayed down with UV/filter-sterilized seawater to cool the blade and wash off any debris, thus reducing cross-contamination between corals. The healthy coral colonies of the following species were sampled for MS-based metabolomics analysis: *Meandrina meandrites* (n=5), *Colpophyllia natans* (n=3), *Montastraea cavernosa* (n=4), and *Orbicella faveolata* (n=4). For each of these corals, a sample of surface mucus and tissue was also collected with a sterile 60 ml syringe by agitating and scraping the coral surface while drawing the dislodged coral tissue into a syringe. Excess seawater was removed from the syringes and these samples were transferred to 15 ml conical tubes. Coral pieces and syringe samples were immediately frozen (-80 °C) followed by freeze drying the samples the next day. All corals were then measured, weighed and extracted twice in the 2:2:1 ethyl acetate:methanol:water solvent mixture in Dr. Paul's laboratory. Extractions were dried by rotary evaporation and Speed-vac and weighed. Having both the surface mucus/tissue extracts as well as the extracts of whole colonies will be valuable for method development. We expect metabolites to be present in the whole coral extracts that are not present in the surface tissues because corals have a layer of endolithic algae and microbes including fungi in their skeleton under the coral tissue that should have its own metabolomic signature. We analyzed whole coral samples, skeleton tissue and surface mucus/tissue extracts from the same colonies using the LC-MS based methodology developed above for bacteria isolated from corals. After generating a FBMN from positive mode MS-data, the features detected in extraction blanks were removed from the network, resulting in a total of 5,721 metabolite features. As expected, whole coral samples represent majority of the features detected. Of all features, 1,024 metabolite features

were shared between all sample types, while whole coral samples contain the greatest number of unique features (Fig. 29). Skeleton samples have 474 unique features, while mucus samples have 211 unique features. When comparisons between healthy and diseased samples are made, such analysis will be beneficial in determining the regions where disease phenotypes are manifested at the metabolite level.

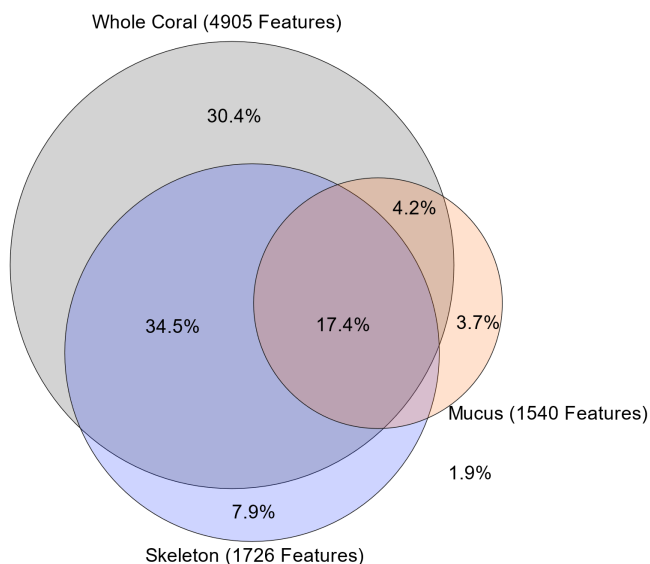


Figure 29. A Venn-diagram representation of overlap of metabolite features detected in corals collected from Dry Tortugas. The percentages reported are based on detection of total 5,721 metabolite features after deletion of features detected in blanks.

Next, we queried how much of the detected metabolome is unique or shared between different species of corals analyzed (Fig. 30). Herein, 1,733 of the features (30.3% of all detected features) are shared amongst all four species with *M. cavernosa* displaying the greatest number of unique features (9.1%). We will use analysis shown in Figures 29 and 30 to guide future feature annotations.

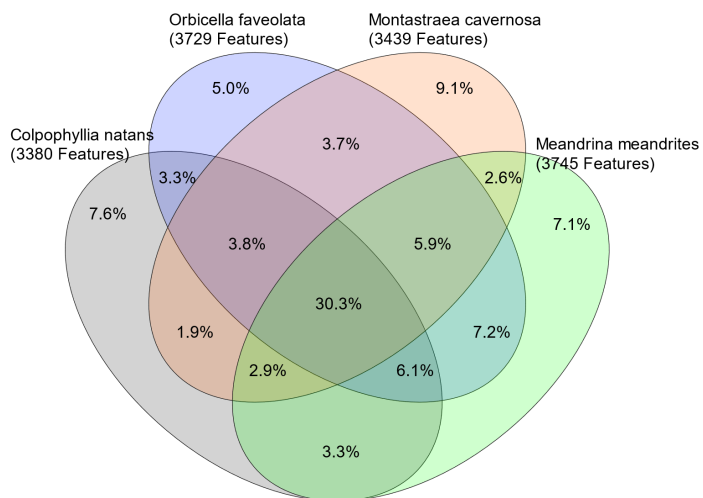


Figure 30. Dry Tortugas Features by Coral Species. A Venn-diagram representation of overlap of metabolite features detected in different species of corals collected from Dry Tortugas.

Structural annotation of detected metabolite features. First, we began annotation of lipids that have been previously reported in metabolomics studies of corals and distinguished resilient corals from bleached corals or diseased corals from healthy corals. Recently, betaine lipids were identified as important metabolites distinguishing resilient corals from bleached corals. Betaine lipids were detected across all sample types and coral species from the Dry Tortugas.

Lipid platelet activating factor (PAF) and its inactive form Lyso-PAF have been implicated in the immune response of corals, and a high concentration of Lyso-PAF has been reported in non-bleached corals. GNPS suggests the presence of Lyso-PAF C-18 in all coral species tested, which is expected in healthy samples based upon previous findings.

Pheophorbide, a zooxanthellae-produced chlorophyll degradation product, has been previously detected in non-bleached corals. Such compounds are of interest due to their anti-inflammatory and antioxidant properties. Features in the LC/MS could be assigned as pheophorbide, supported by the annotation of fragment peaks in the MS² spectra, and a methylated analog was assigned as well. Fucoxanthin, a carotenoid synthesized by marine macro- and micro-algae with known antioxidant properties, was also detected.

Metabolomics analysis of healthy and diseased *M. cavernosa* species coral. On January 16, 2020, 29 samples of *M. cavernosa* were collected on a reef near Hollywood, Florida by a team led by Dr. Paul. These samples were collected under Florida Fish and Wildlife Conservation Commission Special Activity License SAL-19-2201-SRP to Dr. Paul. These were collected by syringe sampling as previously described. Eight corals had active disease, and samples of diseased lesions and healthy portions on the opposite side of the same colony were sampled separately. Thirteen apparently healthy colonies with no visual disease signs were also sampled. Excess seawater was removed from the syringes and coral surface tissue samples were transferred to 15 ml falcon tubes and immediately frozen (-80 °C) followed by freeze drying the samples the next day. The diseased corals were subsequently treated that same day (after the syringe sampling) by the probiotic bacterium *Pseudoalteromonas* sp. MCH1-7 as part of an experiment designed to test whether the probiotic can be an effective treatment against SCTLD. All corals were sampled again in the same way on January 30, 2020, and all samples were frozen and freeze dried. Samples from both dates have been extracted by our standard extraction methods, dried, and weighed. These will be important samples for determining baseline metabolomes of *M. cavernosa* from Broward County reefs, for comparing metabolomes of diseased and healthy portions of the same colony, and for determining whether a metabolomic signature can be detected for MCH1-7 in the probiotic-treated corals.

Next, we employed partial least squares-discriminate analysis using MetaboAnalyst on samples collected on January 16, 2020 to build a model that can differentiate between healthy and diseased corals and to rank metabolite features, the abundances of which separate the diseased corals from healthy corals. Pareto scaling was used, with no sample normalization and no data filtering applied beyond the default setting of the MetaboAnalyst program. The healthy and diseased samples

separate into two groups with 16.9% of the variation explained by component 1, 9.6% of the variation explained by component 2, and 6.6% explained by component 3 (Fig. 31).

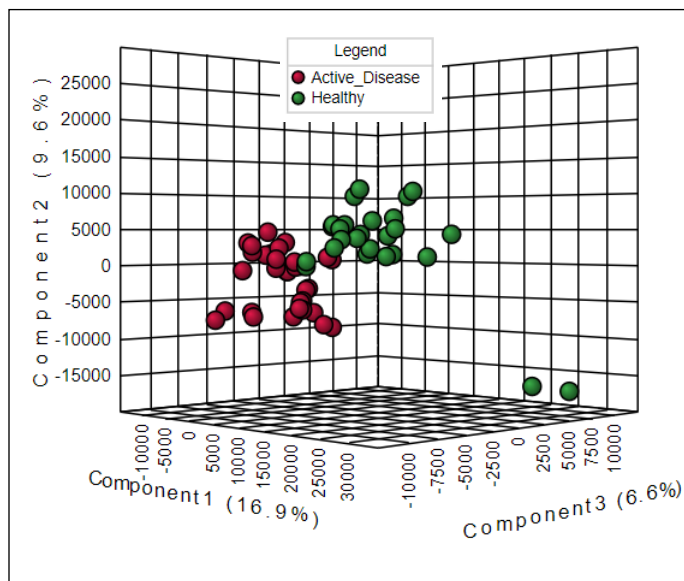


Figure 31. 3D Score Plot of the selected components. The variance between healthy and actively diseased coral samples explained by each component is in brackets.

The Variable Importance in Projection (VIP) plot generated from this model reveals key metabolites that differentiate the diseased state of the sample (Fig. 32). On-going efforts are focused on identifying these metabolites using the in-silico tools and methods previously described.

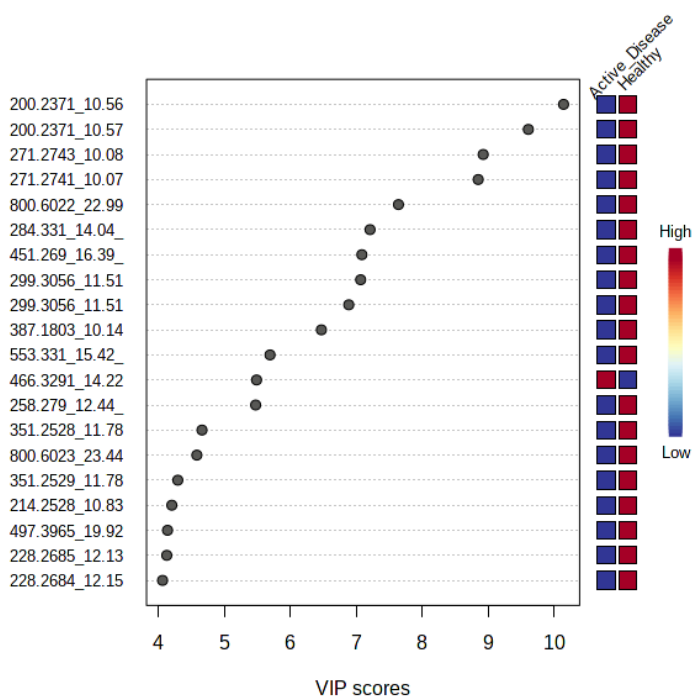


Figure 32. VIP Plot for Healthy vs Diseased Coral Samples. Each feature is reported on the left axis as m/z RT (min). The right axis shows the relative intensity of each feature in active disease samples and healthy samples. Most features that differentiate the samples in this model are detected in higher abundance in healthy coral samples. The notable exception is feature m/z 466.3291, RT 14.22 min.

Lastly, the detected metabolite features were uploaded to the SIRIUS platform, CANOPUS was used to assign compound classes to the 925 features in the dataset and the classes were tested using Mann-Whitney *U* test for overrepresentation (Figure 33 and 34). The healthy corals were found to have a greater representation of natural products such as triterpenoids, hydroxysteroids, benzenoids, etc. as well as lipids and amino acids and derivatives (Fig 33). A similar analysis conducted for diseased corals reveals a higher representation of prostaglandins and steroids (Fig. 34). Prostaglandins are group of lipids that are produced at the site of infection and represent an organism's response to infection or injury. Their overrepresentation during disease further supports the feasibility of our approach to generate biomarkers for diagnosis of SCTLD. The future analysis will focus on annotation of the compounds in these molecular families. These results were presented during the disease advisory call for SCTLD and are informing future treatment trials of corals with anti-inflammatory molecules such as azithromycin and steroids.

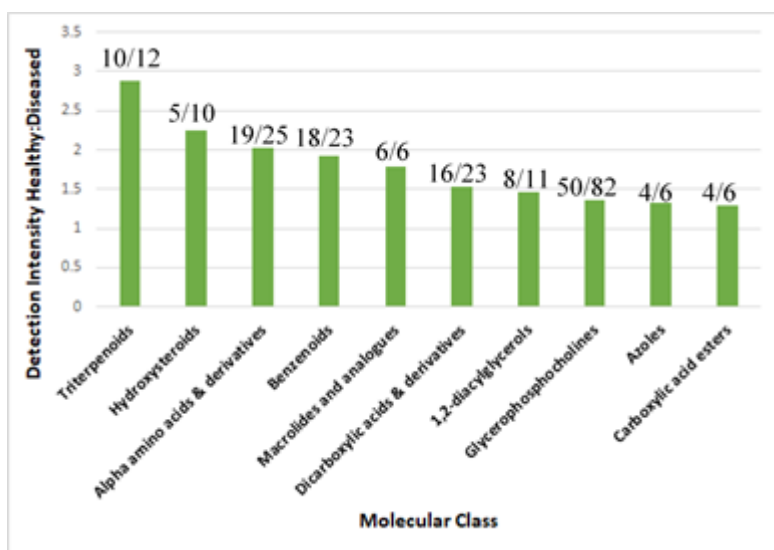


Figure 33: A bar graph of statistically significant molecular classes overrepresented in healthy corals is shown. At least 5 MS-features must be predicted by SIRIUS/CANOPUS and a p-value < 0.05 from Mann-Whitney *U* Test for the molecular class to be considered as differentiating between healthy and diseased samples. The first ten molecular classes that fit these parameters are displayed. The number of metabolite features detected in higher abundance in healthy corals as compared to total number of features proposed for each molecular class is shown on the top of each bar.

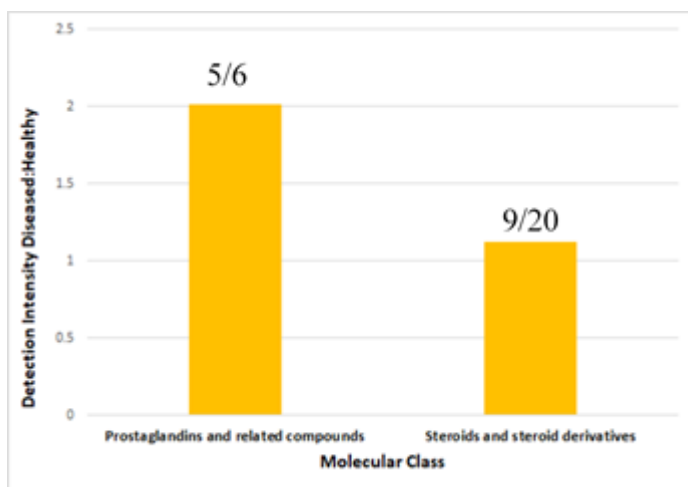


Figure 34: A bar graph of statistically significant molecular classes overrepresented in diseased corals is shown. At least 5 MS-features must be predicted by SIRIUS/CANOPUS and a p-value < 0.05 from Mann-Whitney *U* Test for the molecular class to be considered as differentiating between healthy and diseased samples. The number of metabolite features detected in higher abundance in healthy corals as compared to total number of features proposed for each molecular class is shown on the top of each bar.

Results summary and future directions:

- **A total of 400 out of 2,000 isolates show antibacterial activity against putative pathogens**
- **Chemical analysis of McH1-7 and Of7M-16 shows they both produce three different antibacterial compounds**
- **McH1-7 has proven effective at treating *M. cavernosa* colonies but is less effective with *C. natans* and possibly *P. strigosa***
- **Significant slowing of the disease process on *C. natans* does suggest that probiotics are a possible treatment, but more species-specific strains are needed**
- **Of7M-16 does not seem effective at treating infected *O. faveolata* or *M. cavernosa* colonies and will no longer be pursued as a probiotic treatment**
- **Combinational probiotic treatments have not yet been more successful than McH1-7 at treating SCTL D; different combinations will be pursued in the future**
- **Essential oils may not be a safe alternative treatment for SCTL D as they appear to cause harm to the coral fragments and will no longer be pursued**
- **The presence of *Vibrio coralliilyticus* on disease lesions is associated with faster lesion progression rate and mortality on *M. cavernosa* regardless of location along the FRT. Probiotics with the ability to combat this bacterium will be targeted in the future**
- **Metabolomics has been an important advance to speeding up the identification of known antibiotics in our probiotic bacteria and identifying compound classes that may be biomarkers for SCTL D**